

www.acsami.org Review

Quantitative Advantages of Corrosion Sensing Using Fluorescence, Microscopy, and Single-Molecule Detection

Mark Siegel, Lianlian Liu, Zechariah Pfaffenberger, and Lydia Kisley*



Cite This: ACS Appl. Mater. Interfaces 2024, 16, 56481-56496



ACCESS

III Metrics & More

Article Recommendations

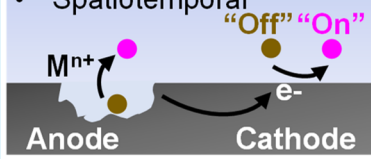
SI Supporting Information

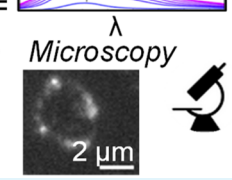
ABSTRACT: The corrosion of metals and alloys is a fundamental issue in modern society. Understanding the mechanisms that cause and prevent corrosion is integral to saving millions of dollars each year and to ensure the safe use of infrastructure subject to the hazardous degrading effects of corrosion. Despite this, corrosion detection techniques have lacked precise, quantitative information, with industries taking a top-down, macroscale approach to analyzing corrosion with tests that span months to years and yield qualitative information. Fluorescence, a well-established optical method, can fill the niche of early-stage, quantitative corrosion detection and can be employed for both bulk and localized testing over time. The latter, fluorescence microscopy, can be pushed to greater levels of detail with single-molecule

Sensing corrosion with fluorescence:

• In situ

• Chemical specificity: pH, metal ion, e
• Spatiotemporal





microscopy, achieving nanometer spatial and subsecond temporal resolutions of corrosion that allow for the extraction of dynamic information and kinetics. This review will present how fluorescence microscopy can provide researchers with a molecular view into the chemical mechanisms of corrosion at interfaces and allow for faster, quantitative studies of how to detect and prevent corrosion.

KEYWORDS: corrosion, fluorescence, optical microscopy, metal interfaces, smart sensors, coatings, quantitative sensors, single-molecule microscopy

1. INTRODUCTION

Metal corrosion, a spontaneous interfacial degradation process, results in an estimated U.S. \$2.5 trillion in global spending every year, which accounts for 3.4% of the global GDP and can lead to major human safety concerns and environmental consequences. 1,2 The costly and dangerous consequences of leaving corrosion unchecked have motivated the development of techniques for corrosion detection. However, corrosion detection in many industries relies on inefficient methods that provide minimal quantitative information, take months to years to yield results, and cannot detect corrosion at very early stages.^{3,4} Longer timescale, qualitative tests make it difficult for industries to appropriately test corrosion prevention techniques and hinder the progress to lessen the costly effects of corrosion. An ideal detection method would be able to detect corrosion at much shorter time scales (<hours) in addition to longer time scales (days and beyond) and provide quantitative information on corrosion kinetics in an in situ dynamic

A wide array of techniques has been employed to detect corrosion (Table 1), each with distinct benefits and disadvantages. A common corrosion measurement is immersion testing, in which mass measurements of a sample are taken before and after corrosion occurs.⁵ Immersion tests can quantify corrosion rates after a long-term immersion

(commonly more than 1 week for stainless steels) but provide little information on the fundamental principles that initiate and propagate corrosion. Other detection methods are limited to simpler results that show whether corrosion has occurred or not including acoustic emission,⁶ thermal imaging,⁷ and ultrasonic inspection.^{8,9} Electrochemical methods like interferometric techniques, ¹⁰ local electrochemical impedance spectroscopy (LEIS), ^{11–13} and scanning electrochemical microscopy (SECM) 14,15 quantify electrochemical properties of corrosion efficiently. However, electrochemical techniques require an external stimulation, such as applied potential or charge, to drive the corrosion processes, preventing the analysis of naturally occurring corrosion as it would occur outside the laboratory setting. Additionally, these techniques fail to break past resolutions smaller than micrometer resolutions. Several microscopic techniques can obtain submicrometer resolutions, such as atomic-force microscopy (AFM), or scanning electron microscope (SEM), 17,1

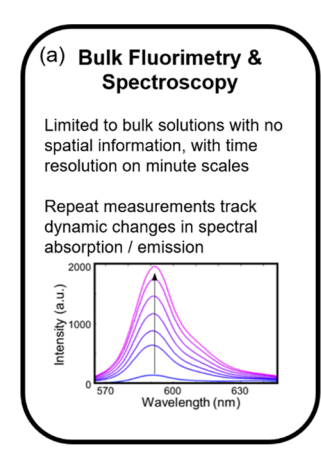
Received: May 12, 2024
Revised: September 18, 2024
Accepted: September 23, 2024
Published: October 11, 2024





Table 1. Comparison of Various Corrosion Detection Techniques

Detection Technique	Corrosion Sample Conditions	Spatial Resolution	Benefits	Limitations	Resulting Data	ref.
Immersion Testing	Variable. In situ, ex situ, native, and electrochemical environments	N/A (bulk)	Cheap and easy to perform	Tests can take months to years	Comparison of mass before and after corrosion	8
Acoustic Emission	Metal sheets on cm scale, in situ	100 µm	Sensitive to rapid crack propagation. Can be done in tandem with electrochemical tests	Limited to large area $(mm^2 \text{ to } 100 \ \mu\text{m}^2)$ deformations	Acoustic signals generated by metal degradation	9
Thermal Imaging	Thin metals, in situ	Single mm	Noninvasive hidden corrosion detection	Inaccuracy can reach 20%, struggles above 5 mm thickness, resolution in mm	IR images	7
Ultrasonic Inspection	Back surface of plate-like structures, in situ	100s of μ m	Noninvasive, nondestructive back surface corrosion detection	Detection limited to larger signs of corrosion (thickness change of 0.1 mm or more)	Ultrasonic signal changes/ surface roughness	8, 9
Interferometric Methods	In situ electrochemical environments	Single μ m	Provides accurate information on physical geometry of samples	Resolution limited to μm scale	Images, topographical maps, material dissolution flux values	10
LEIS	In situ electrochemical environment	10s of μm	Redox mediator not required in solutions	Resolution limited to 10s of μm	Local impedance, electrochemical information	11–13
SECM	Electrochemical environments	100s of nm	Window into electrochemical activity of sample	Slow imaging speeds, thus poor temporal resolution. Resolution in μ m range	Map of electrochemical activity	14, 15
AFM	Variable, ex situ	Single nm	Resolution down to single nm	Limited dynamic information, analyzes a limited area of sample.	3D surface profile, topological information	16
SEM	Static, ex situ imaging postcorrosion	Single nm	Single nm resolution, local elemental makeup (EDS)	Limited dynamic information and electron beam may interfere with corrosion mechanisms	Static images, elemental makeup	17, 18
TEM	In situ corrosion in gaseous, liquid, and electrochemical environments or ex situ imaging	10s of nm	Resolution on nm range	Electron beam may interfere with corrosion mechanisms	Static images, electrochemical information over time	19
UV-vis Absorbance	Variable. In situ, ex situ, native, and electrochemical environments	N/A (bulk)	Wide variety of testing applications	Limited sensitivity and limited ability to measure dynamic properties.	Bulk solution spectra	20, 21



(b) Diffraction-Limited Fluorescence Microscopy In situ corrosion imaging with 200-300 nm spatial resolution and ms temporal resolution compatible with electrochemical techniques Sample dynamics observable over

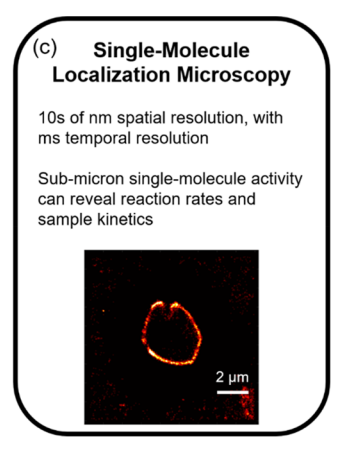


Figure 1. Highlights of corrosion detection using various fluorescence techniques. (a) Intensity increase over time of fluorophore resazurin reducing into resorufin in the presence of corroding metal. 28 (b) Corrosion of an iron colloid detected by fluorescent resorufin. (c) SMLM image of fluorescent resorufin around the same iron colloid as (b).

which can further use energy dispersive spectroscopy (EDS) to quantify local elemental makeup, and transmission electron microscopy (TEM), 19 which allows for in situ measurements. These microscopy methods still have their own drawbacks, however. AFM, for example, results in 3D surface profiles with topographical information on the roughness of samples down to nanometer precision, but is somewhat slow to perform due to the point nature of the detection, provides little information on dynamic changes in chemical processes over time, and is limited to lateral areas of interest of 150 μ m \times 150 μ m. SEM and TEM imaging techniques can provide nanometer resolutions as well, but SEM is generally limited to analyzing static samples rather than actively observing corrosion as it happens due to the vacuum environment of the sample chamber. TEM and SEM also risk interfering with corrosion processes via their incident electron beams used to image samples. Ultraviolet-visible spectroscopy (UV-vis) absorption techniques, on the other hand, are good methods to probe corrosion properties, and do not rely on detection methods that could interfere with corrosion processes. 20,21 However, UV-vis tests in practice predominantly focus on bulk testing and therefore cannot provide any information regarding local corrosion sites and properties, as sites corrode over time.

Fluorescence spectroscopy and microscopy are in situ techniques that provide a plethora of qualitative and quantitative information when applied to corrosion detection. Many fields use fluorescence microscopy as a primary detection and imaging tool, such as biology, 22-24 medicine, 25 and environmental sciences. Fluorescence offers high sensitivity, efficiency, and versatility, while combining the variety of test parameters of spectroscopic techniques with microscopy provides localized spatial precision. As a brief review, fluorescence detection techniques are based around exciting certain molecules, called fluorophores, with wavelengths of light that cause an electron of the fluorophores to jump to a higher electronic energy level.²⁷ The electron then nonradiatively loses some vibrational energy in the excited state, followed by the process of the electron dropping back down to the ground energy level by radiatively emitting a photon with lower energy than the photon that excited it, which is called a Stokes shift. The Stokes shift allows the emitted fluorescence to be analyzed independent of the excitation light used, allowing for clear isolation of the signal. Fluorophores can be designed to "turn-on" or "turn-off" when

in the presence of experimental factors of interest. Corrosion is such a factor, and certain fluorophores can be activated or quenched when they undergo reduction or oxidation reactions in an actively corroding environment. ^{28–37} Other fluorophores used to detect corrosion include those that display sensitivity to different levels of pH^{38-60} and those that exhibit changes in fluorescence when exposed to metal ions.⁶¹⁻⁶

Fluorophores can be applied in both spectroscopic and microscopic setups. Bulk fluorescence is an accessible method using common laboratory spectroscopic equipment, but the sensitivity can be difficult to analyze on time scales below minutes and cannot report any localized information. The limitations of cuvette-based spectroscopy can be overcome using standard microscopy experiments to image fluorophores on corroding surfaces, but these in turn are limited in spatial resolution due to the diffraction limit of light.⁶⁸ One approach that could propel fluorescence-based corrosion detection to new levels of quantitative detail is single-molecule localization microscopy (SMLM), which can provide kinetic information on localized corrosion reactions at nanometer spatial and millisecond temporal resolutions. $^{32,69-74}$

This review will address why fluorescence techniques are powerful tools for detecting corrosion in a variety of different applications (Figure 1). We will begin by discussing the mechanisms of the fluorescence sensing of corrosion products (section 2). We then review a variety of techniques that apply fluorescence to the study of corrosion, including bulk measurements and microscopy (section 3). Finally, we will address how fluorescence microscopy can be pushed further with the adaptation of SMLM to study corrosion at a more fundamental level than ever before, allowing for nanometer spatial and subsecond temporal resolution studies that provide meaningful, quantitative insights into in situ corrosion dynamics and kinetics (section 4).

2. MECHANISMS OF FLUORESCENCE-BASED CORROSION DETECTION

Corrosion is a spontaneous electrochemical degradation process occurring at a metal/environment interface, where oxidation of the metal occurs at anodic areas and the reduction of environmental species occurs at cathodic areas (Figure 2).75 At the anode, metal dissolution and the subsequent hydrolysis reactions result in metal ion accumulation in solution and localized acidification, while at the cathode, localized

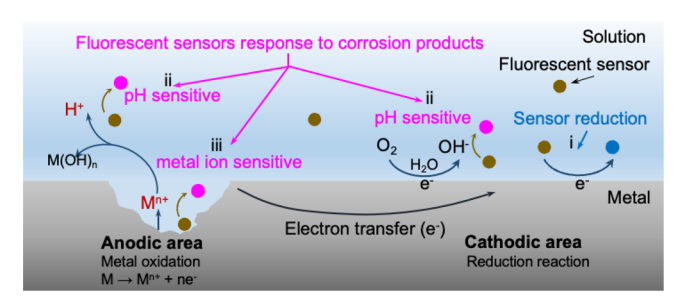


Figure 2. Schematic of fluorescence-based corrosion detection mechanisms at a metal/solution interface via (i) electrochemical sensors, (ii) pH-sensitive sensors, and (iii) metal ion-sensitive sensors.

alkalization is caused by the reduction reaction of water and oxygen. Fluorescent indicators can probe corrosion in both anodic and cathodic areas by being (i) directly involved in the electrochemical reactions, (ii) sensing the pH variations, or (iii) probing the metal ions in the environment.

2.1. Electrochemical Fluorescent Sensors Indicate Corrosion via Redox Turn-On. Electrochemical fluorescent sensors have been reported to sense corrosion in cathodic areas by taking part in reduction reactions (Figure 2i, blue). For instance, we have applied resazurin to characterize iron corrosion in aqueous solutions at the single-molecule level, 29-31 and to study the time-dependence of corrosion in organic-based solutions including ethanol and acetone. 28,32,33 Resazurin is a henoxazin-3-one dye with weak fluorescence (emission quantum yield, $\phi = 0.11$), that can then be irreversibly reduced to strongly fluorescent resorufin (ϕ = 0.74) (Figure 3a). 28,29,34,35 The intramolecular charge transfer (ICT) from the electron donating group (-NH₂) HOMO to the electron acceptor LUMO contributes to the strong fluorescent emission of resorufin. 34,35 However, the covalent coordinated oxygen in resazurin restricts the group from acting as an electron donor, suppressing the ICT interaction between the electron donor and acceptor, and quenching the emission, seen in Figure 3a.

Amplex red is another electrochemical fluorescent dye related to resorufin. The covalently bonded acetyl group $(-CO-CH_3)$ diminishes the ICT interaction, quenching the fluorescence. Different from the reduction turn-on of resazurin, weakly fluorescent Amplex red is irreversibly oxidized to resorufin as shown in Figure 3b.³⁶ This oxidation turn-on of Amplex red has been applied to spatially resolve the electrochemical process on the surfaces of electrodes and nanocatalysts.^{36,37}

2.2. pH Sensors Detect pH Variation Caused by Metal Corrosion. pH sensors can probe corrosion by responding to anodic acidification or/and cathodic alkalization theoretically down to single-molecule limit. BH sensing dyes can modify absorption (color) or fluorescent properties (emission turnon/quenching and/or spectral shift) with pH (Figure 4). Phenolphthalein, neutral red, bromocresol green, phenol red, bromothymol blue, and cresol red are the pH-triggered color change sensors commonly used in coatings to report underfilm metal corrosion. However, the applications of pH-triggered color change sensors in underfilm corrosion detection have been restricted by adding pigments. Therefore, this work focuses on fluorescent pH sensors.

Fluorescent pH sensors have different protonated (acidic) and deprotonated (basic) forms with distinct fluorescent properties depending on the dissociation constant pK_a at different pH values (Figure 4b). 40,46,47 For example, fluorescein, a triarylmethane-based dye, has multiple ionization equilibria associated with pH dependent emission over the pH range of 5 to 9 (Figure 4c). 48 The photoinduced electron transfer (PET) from the benzene ring to the xanthene moiety has been widely accepted to explain the fluorescence turn-on with increasing pH. However, Zhou et al. have contributed the fluorescein turn-on in alkaline conditions to the formation of a minimal energy conical intersection (MECI), which involves rotation of the benzene ring and a flip-flop motion of the xanthene moiety. These motions are restricted by intermolecular hydrogen bonding.⁴⁹ Though the mechanism of fluorescein sensing pH variation has not been fully understood yet, fluorescein and its derivatives have been applied to sense aluminum corrosion at early stages in both solution and in coating systems. 41,50-54 An example of fluorescein derivative, 5,6-carboxyl fluorescein (56CF) sensing pH reduction caused

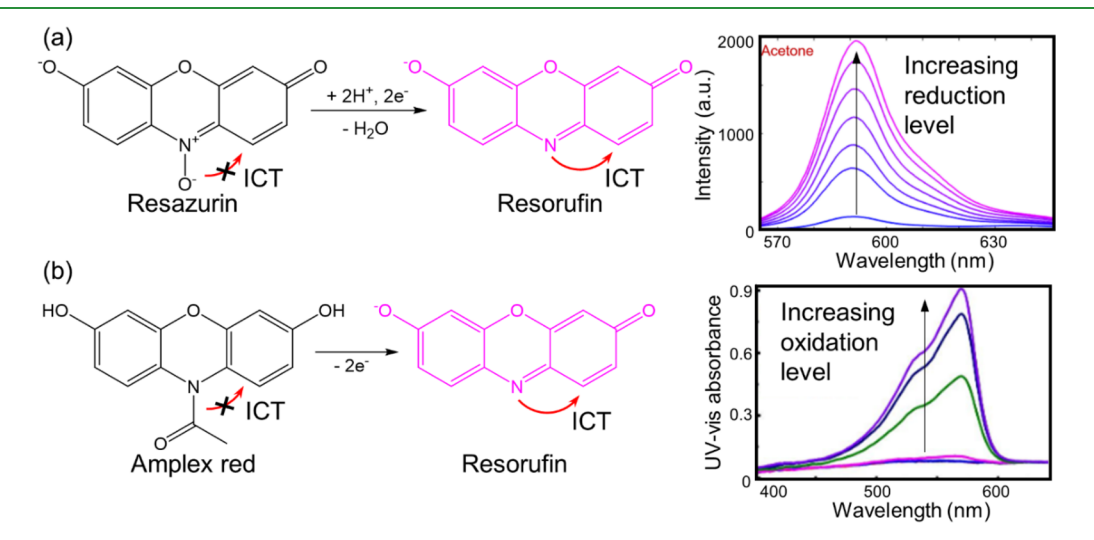


Figure 3. Electrochemical sensor shows redox turn-on due to existence of ICT from electron donor ($-NH_2$) to the rings. (a) Reduction turn-on of resazurin with example emission spectra of resorufin sensing metal corrosion in acetone. (b) Oxidation turn-on of Amplex red with example emission spectra of showing 10 μ M Amplex red in 10 mM phosphate-buffered saline (PBS) to sense electrochemical processes on Au microelectrode via fluorescence lifetime imaging microscopy (FLIM). Reproduced from ref 36. Copyright 2023 American Chemical Society.

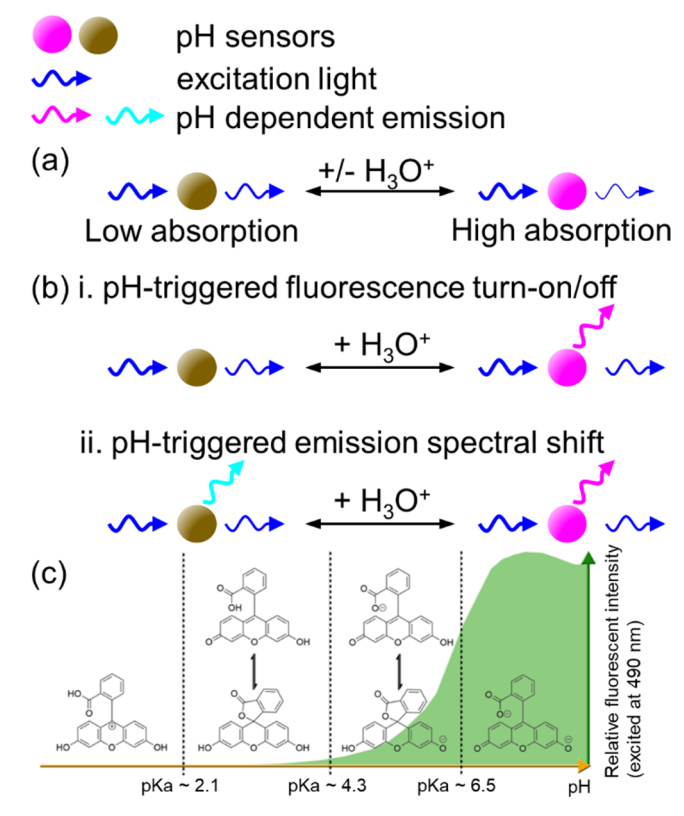


Figure 4. Schematic of optical pH sensor mechanisms. (a) Absorption (color) modification of a sensor with pH. (b) Fluorescent pH sensors experience fluorescence (i) turn-on and/or (ii) change via binding with hydrogen ions. (c) Fluorescein has different protonated (acidic) and deprotonated (basic) forms with distinct fluorescent properties depending on pH values. Fluorescein derivatives are quenched in acidic environments. Reproduced from ref 48. Available under CC-BY license. Copyright 2020 by Le Guern, F.; Mussard, V.; Gaucher, A.; Rottman, M.; Prim, D. An example of fluorescein derivative 56CF senses localized corrosion on an iron surface is further exhibited in Figure 9a.

by localized corrosion, is reported in Figure 9a and will be further discussed in section 3.55 Like fluorescein, most of the pH fluorescent sensors turn-on after exposure to alkaline environments at cathodic areas of the corrosion process, such as coumarin and its derivatives, 56-59 while TPM ((E)-N-(1H-indazol-3-yl)-1-(4-(1,2,2-triphenylvinyl)phenyl)menthanimine) shows fluorescence turn-on in acidic environments at anodic areas. 60

2.3. Metal Ion Sensors Detect Corrosion via Chelation-Enhanced Mechanisms. Metal ion fluorescent sensors can be used to study the anodic dissolution of corrosion processes. A classical fluorescent sensor for metal typically has two components: (1) one or more fluorophores that are covalently bonded to (2) a metal-coordinating portion of the molecule by a spacer. The coordinating active portion can bind with metal ions and cause either fluorescence turnon/quenching or a spectroscopic shift, or both, depending on the fluorescence principles shown in Figure 5.61 For example, after binding with metal ions, sensors with a PET mechanism (Figure 5a) undergo fluorescence turn-on, also called chelation enhanced fluorescence (CHEF), while those with ICT show chelation enhancement quenching (CHEQ) (Figure 5b). Other mechanisms displayed in Figure 5c-e, including fluorescence resonance energy transfer (FRET), excimer

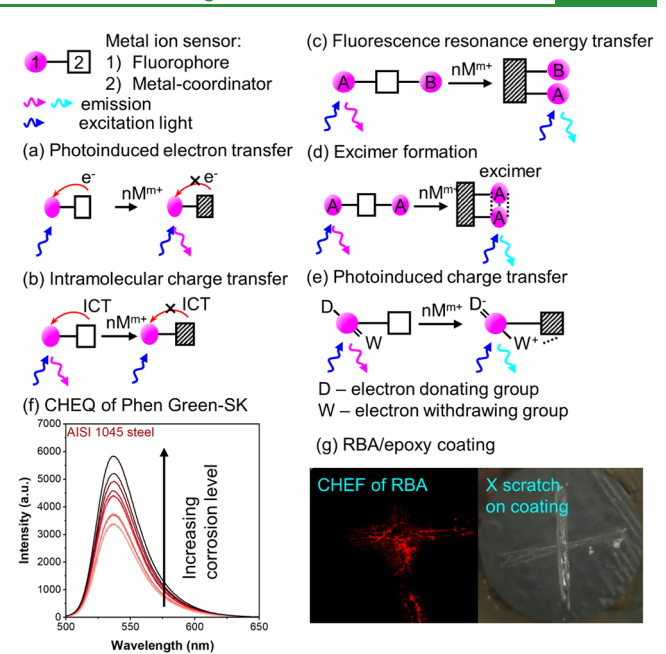


Figure 5. Mechanisms of metal ion sensors. Sensors with (a) PET mechanism show fluorescence turn-on (CHEF) after chelating with metal ions; with (b) ICT mechanism are quenched by metal ions; with (c) FRET, (d) excimer formation, and (e) PCT mechanisms experience both emission intensity variation and spectral shift. (f) Example spectra of PGSK senses carbon steel corrosion in ethanol-based solution, PGSK experiences ICT CHEQ (fluorescence turn-off) after binding with metal ions. Reproduced from ref 67. Available under CC-BY licenses. Copyright 2024 Liu, L.; Pfaffenberger, Z.; Siegel, M.; Saini, A.; Kisley, L. (g) An example of a metal ion sensor sensing under-coating corrosion: Rhodamine B acylhydrazone (RBA) in epoxy coating detects under-coating iron corrosion, RBA show CHEF (fluorescence turn-on) after binding with Fe³⁺. Adapted with permission from ref 21. Copyright 2021, Elsevier. Note: the line-filled metal-coordinator means the sensor binds with metal ion(s).

formation, and photoinduced charge transfer (PCT), can cause both emission intensity and wavelength changes. Formica et al. have reported different principles in more detail.⁶¹ Metal sensors with PET and ICT fluorescence mechanisms have been widely used to detect metal ions created by corrosion. For instance, 8-hydroxyquinoline (8-HQ) and its derivatives have been reported to sense undercoating aluminum and carbon steel corrosion at early stage by PET turn-on. 42,62,63 Rhodamine derivatives reported as a complex forming ligand with transition metal ions to display fluorescence, and therefore have been introduced in a coating system to monitor the corrosion of copper- and iron-based alloys. 21,21,64,65 Phenylfluorone (PF) has been used as CHEQ sensors in coatings to monitor aluminum corrosion. 66 Aside from coatings, metal ion sensors have been applied to corrosion detection in solution. In our own lab, Saini et al. sensed iron corrosion in water by FeRhoNox-1 and FluoZin-3 turn-on (CHEF) and Liu et al. developed a methodology to quantify metal corrosion from Phen Green-SK (PGSK) quenching (CHEQ) in an ethanol-based solution. 6

2.4. Challenges of Using Fluorescent Sensors for Corrosion Detection. Aside from the sensing mechanism, a range of other specifications of fluorophores should be considered before their application in corrosion sensing and mapping. These properties include sensor sensitivity, operational and storage stability, response time, accuracy, precision,

operating temperature, required sensor resolution, toxicity of the materials, and the diffusion in and interaction with environments (solution, coating, etc.). An ideal sensor (1) should have high sensitivity and short response time to electron transfer, pH, and metal ion variations caused by corrosion, (2) can sense the corroded area precisely at high resolution or at the single-molecule level, (3) has fluorescence turn-on with high quantum yield and enough lifetime and resident time at the metal/solution interface for single-molecule detection, (4) does not affect the corrosion, or at least not accelerate the corrosion process, and (5) has no side reactions or interactions with surroundings.

However, the mentioned sensors cannot satisfy all the requirements and have limitations in corrosion detection. For example, resorufin can be further reduced to nonfluorescent dihydroresorufin, and this side reaction can lead to an underestimation of metal corrosion. Furthermore, pH sensors may experience premature fluorescence turn-on in an alkaline resin coating. In addition, the applications of metal ion sensors in single-molecule corrosion detection are rare due to the low quantum yields of metal ion sensors and the complex interactions between the fluorophore with the surrounding solvent. Metal ion sensors have further been observed to have undesired reactions from other corrosion products that can give false sensing of a metal ion, such as the irreversible hydrolysis of an Fe³⁺-chelating fluorophore by H⁺ present at the acidic anodic sites.⁷⁶

There are other sensors that have been introduced in the single-molecule bioimaging and catalysis fields, which have the potential to be applied to corrosion detection. For instance, methylene blue and BODIPY can be quenched by reversible electron transfer from the reductant to act as reduction "turn-off" dye sensors. The Many works have verified the efficiency of these sensors in imaging electro- and photocatalysis by single-molecule fluorescence microscopy. The Standard Sta

3. CURRENTLY USED ANALYTICAL FLUORESCENCE TECHNIQUES

Whether the fluorescent probes are sensing pH variations, metal ions, or redox electrons (Figure 2), the fluorescent sensor must first be introduced to interact chemically with corrosion reaction products, the fluorophore must be excited, and then the emitted light must be detected in some manner. Solutions, coatings, and optical fibers have been used to introduce the fluorescent sensor to the corrosion reaction products, and fluorescence spectrometers or light microscopes have been employed as the detectors (Figures 6-9). In most previous studies, the emitted light has generally been treated as a binary "on" or "off" response. Yet, quantitatively, the magnitude and wavelength of the collected emission signal can be related to the amount or concentration of corrosion products produced over time. Additionally, if the fluorescent signal is imaged on a microscope and camera, the fluorescent signal may report on localized corrosion. Previous studies have been limited temporally to minute or greater scales and spatially to micrometer resolutions.

3.1. Fluorescent Sensors in Solution Allow for Corrosion Rate Measurements. The most straightforward way to introduce a fluorescent probe is by simply placing the

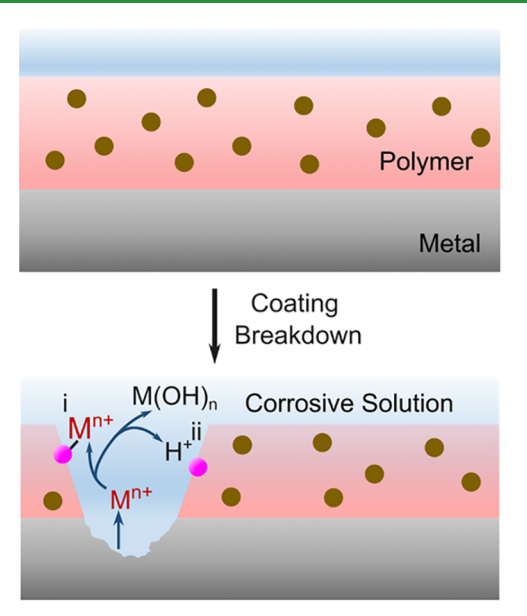


Figure 6. Fluorescent coatings report on localized corrosion. Fluorophores are embedded in a polymer coating. When this coating breaks down, the corrosive solution can access the metal surface. Solvated metal ions (i) or hydrogen ions (ii) will interact with fluorophores exposed from the coating break down and become fluorescent. Brown circles are fluorescent molecules that have not been activated by corrosion products. Solid pink circles are bright fluorescent molecules.

corroding metal in contact with a solution that contains the dissolved fluorescent molecule, which allows quantification of the corrosion rate by measuring the change in fluorescence intensity over time. Our group and others have used this method with a fluorescence spectrometer to quantitively monitor the corrosion rate of metal exposure to solutions over 24 h. ^{28,29,55,67,97} The fluorescent intensity of a solution of resazurin increases over exposure time to an iron powder as electrons transfer from iron to resazurin and converts more resazurin to resorufin, which exhibits strong fluorescence due to ICT (Figure 3a). In particular, our group has sensed differences in the rate of corrosion in different solvents, such as ethanol versus acetone.²⁸ Our solution-based measurements highlight the unique ability of fluorescent corrosion sensors to quantify the corrosion rate in organic environments which is not possible using common electrochemistry-based methods due to the limitations of solution conductivity.

Using a solution-based technique has the following advantages: (1) This method has lower cost. Coatings or optical fibers discussed below need expensive equipment or chemicals that add cost over and above the cost of a fluorescent sensor molecule. (2) This method is very simple. No additional chemical synthesis or complicated optical setups are needed. Commercially available fluorometers can be employed as detectors with nanomolar sensitivities. (3) This method is the least perturbative, as no other materials (such as polymer coatings) contact the metal surface and no electrochemical stimulation is needed as in LEIS and SECM. The simplicity of the solution-based methods leads to its biggest drawback, however. The interaction between the sensor (redox turn-on, pH, or metal ions) and the corrosion products is based on diffusion and thus is random.³¹ Therefore, the interaction is not inherently localized. One must use a detector with a sufficiently fast temporal rate to capture the molecule

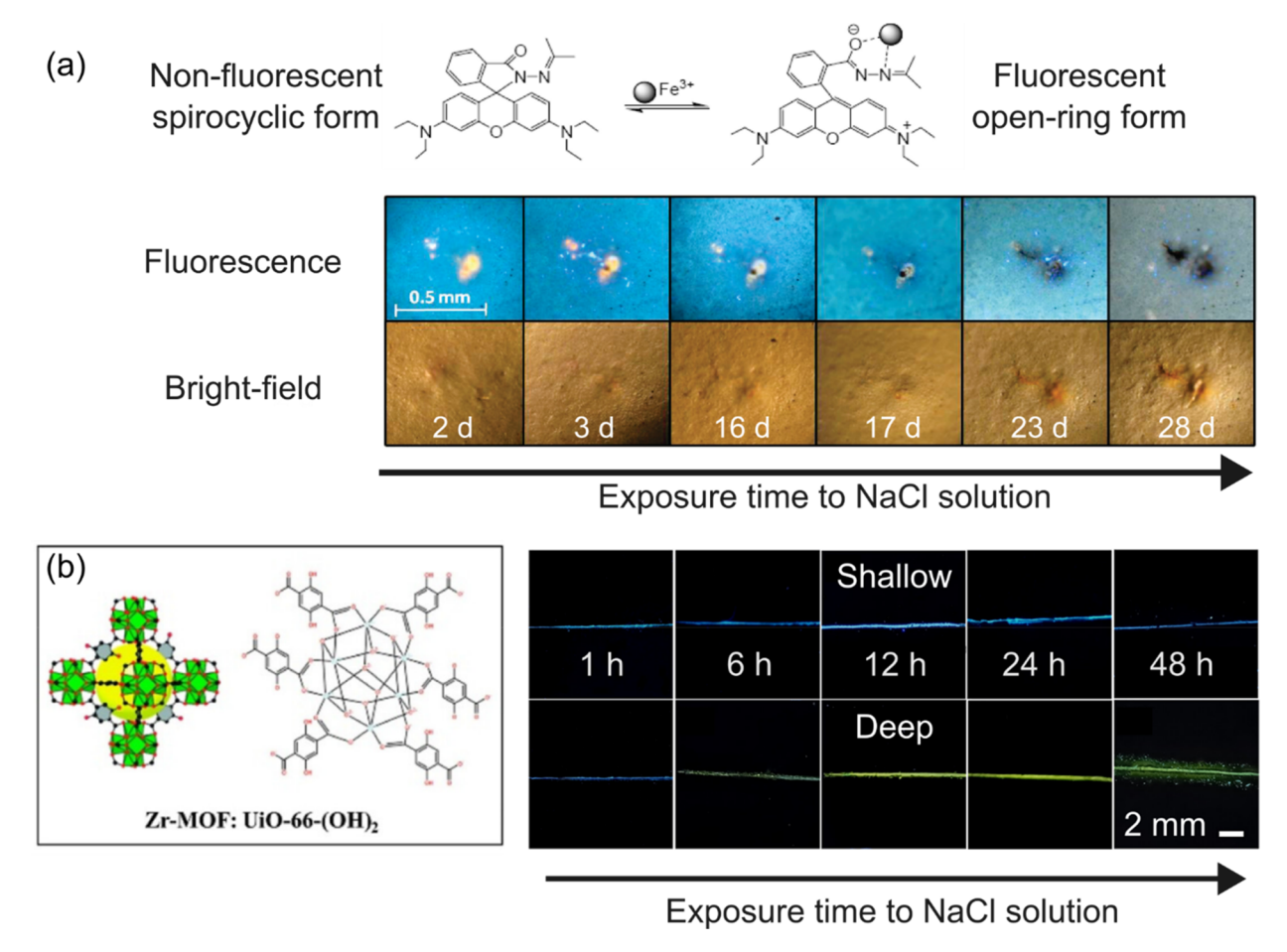


Figure 7. (a) Top: Chemical structure of FD1 in its free form and complexed with Fe³⁺. This sensor is an example of a CHEF. Bottom: Micrographs of FD1 fluorescence were localized to an underfill blister. The dark areas are attributed to corrosion products precipitating out. Reproduced from ref 98. Copyright 2009 American Chemical Society. (b) Left: Zirconium MOF with an embedded quantum dot. The quantum fluoresces blue upon initial breakdown and exposure to a corrosive solution. When the breakdown reaches the metal, the pH increases due to corrosion and the blue fluorescence fades while the yellow fluorescence from the MOF increases. Right: Fluorescence micrographs of shallow and deep scratches were made on carbon steel coated with the Zr-MOF epoxy. Reproduced from ref 100. Copyright 2023 American Chemical Society.

turn-on before it diffuses away from the corrosion site if spatial information is desired.

3.2. Coatings Report on Localized Breakdown and Can Further Protect Surfaces with Release of Anticorrosive Agents. A major research direction in fluorescent corrosion sensors is encapsulating the molecule in a polymer matrix that is coated onto the metal and thus can report on localized sites that corrode. As the coating breaks down, pH sensitive or metal ion sensitive fluorescent molecules become exposed to the solution and can interact with H⁺, OH⁻, or metal ions (Figure 2ii-iii) while remaining immobile at the corrosion site (Figure 6). Localized fluorescent spots reporting corrosion on the micrometer to millimeter length scales have been observed with coating applications. Augustyniak et al. dissolved spiro[1H-isoindole-1,9'-[9H]xanthen]-3(2H)-one, 3',6'-bis(diethylamino)-2-[(1-methylethylidene)amino] (FD1, Figure 7a, top), a sensor that exhibits CHEF upon complexation with Fe³⁺, into a commercially available epoxy polyamide and then cured it onto steel coupons. They applied a drop of silicone oil to mimic undercoating corrosion and observed a localized FD1 fluorescence turn-on. Their technique was limited to detecting corrosion at times earlier than 16 days. After 16 days, the corrosion products precipitated and covered any visible fluorescence (Figure 7a, bottom). The measured

change in fluorescent signal was observed before any changes could be detected by bright-field imaging as seen in the 2-day time point. Additionally, pH sensors have been incorporated into coatings. ^{99,100} Fan et al. developed a zirconium-based metal—organic framework (MOF) with a carbon dot where the fluorescence intensity reported on physical damage to the coating and the color change of the fluorescence reported on the pH change from the corrosion reactions (Figure 7b). ¹⁰⁰ The spectral fluorescence shift allowed the authors to differentiate early-stage coating breakdown and later-stage metal dissolution based on the fluorescent emission color on carbon steel (1 h image version 6–48 h images in Figure 7b).

In addition to localized sensing, a promising direction for coating-based fluorescent sensor research has been smart coatings. Smart coatings serve a dual role, both healing the metal from corrosion and providing early sensing of damage to the coating. For example, 8-HQ has been incorporated into a layer double hydroxide (LDH), acting as both a turn-off fluorescent sensor for aluminum corrosion and releasing 8-HQ which can form an additional protective layer on the surface when and where the coating breaks down. Rhodamine B has also been incorporated into an LDH without reducing the corrosion protective performance of the LDH. In this same study, it was shown that corrosive chloride ions were

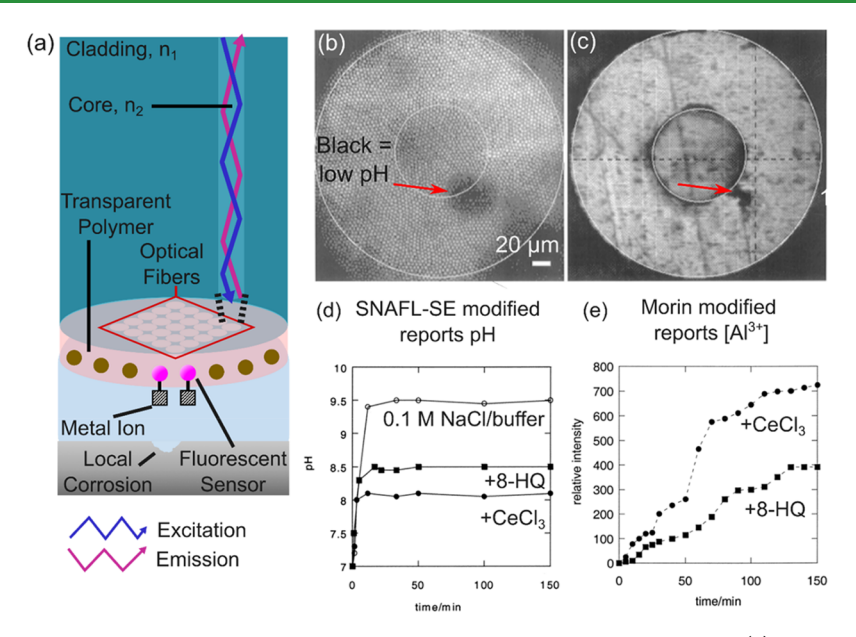


Figure 8. Optical fibers can provide quantitative localized corrosion information but limit spatial resolution. (a) Diagram of an optical fiber that has been modified for fluorescence sensing. (b) Ratiometric fluorescence image from a FITC-modified bundle. Pixelation due to the fibers is visible. (c) Optical micrograph of the same area as (a). (b) and (c) are reproduced from ref 108. Copyright 1997 American Chemical Society. The dark area was visually identified by the authors as corrosion. (d) pH was measured by the ratiometric fluorescence intensity from an SNAFL-SE modified fiber under three different buffer conditions. (e) Fluorescence intensity from a morin modified fiber reporting on the concentration of Al³⁺ vs time. (d) and (e) reproduced from ref 109. Copyright 2002 American Chemical Society.

exchanged with the Rhodamine B upon penetration through the LDH coating protecting the metal from coming into contact with the corrosive agent. Smart coatings have the distinct advantage of releasing corrosion protection in response to a stimuli as needed directly to the most affected areas of the metal. In addition to chemical triggers, certain coatings with photosensitive agents can repair damages to the coating itself upon irradiation with appropriate wavelengths through photothermal effects. Sold Both the previously mentioned study from Fan et al. On and a study from Lee et al. Show that smart coatings can also report on the extent of breakdown. For example, Lee's study used aggregation-induced emission to detect the early crack in the coating before the crack reached the metal and then a pH sensor to report on the acidification once the metal surface was corroding.

Fluorescent coatings have several advantages over other methods of introducing fluorescent sensors. (1) The fluorescence inherently reports on localized corrosion since only breakdown sites are accessible to corrosion products. While resolution and feature sizes have not been quantitatively reported, reported microscopy images show length scales ranging from 100 μ m to 2 mm. 44,98,100,105–107 (2) The coatings inherently protect the metal surface from corroding by preventing corrosive agents from contacting the metal surface. Particularly, the development of smart sensors with dual properties that both sense corrosion and release additional species that can heal corrosion and detect corrosion at early stages the showcase the multifaceted functions of fluorescent coatings. (3) The embedded fluorescent molecules do not immediately diffuse away, simplifying measurements at minutes—hours-long time scales.

Coatings also come with disadvantages for quantifying localized corrosion sizes and rates. (1) The fluorescent signal of molecules can be altered by the coating matrix. For example, rhodamine B was observed to quench prematurely due to the amide group a coating, not from interaction with corrosion

products.²¹ This limitation can be partially overcome by encapsulating the fluorophore in a nanoshell or MOF as in Fan's work, although issues with premature quenching or enhancement have still been observed. 105 (2) Quantification of the concentration of corrosion products down to singlemolecule level is difficult because multiple dyes will be in the vicinity of the film breakdown. (3) The immobilized dyes do not diffuse away, making monitoring ineffective for long time scales. As Augustyniak showed, time scales greater than 2 weeks saw corrosion products cover up the fluorescent signal.98 Together disadvantages 2 and 3 restrict coating applications to temporally monitoring corrosion between minutes on the short end and several days on the long end. (4) If the reaction is irreversible, for example, 8-HQ undergoing CHEF, seen in Figure 3a, then the coating can only be used for corrosion detection once. (5) Because coatings can also alter the corrosion conditions, coatings are less useful for studying fundamentals of corrosion reaction rates and mechanisms because of the additional variables introduced.

3.3. Optical Fibers Enable Localized Imaging of Samples In Situ with Spatial Resolution Limited to the Micrometer Scale. Fluorescent corrosion sensors incorporated into functionalized optical fibers deliver probes to a sample and collect light from the fluorescent sensor molecules after interacting with metal ions, H⁺, or OH⁻ to enable in situ observation (Figure 8a). Optical fibers are plastic or glass fibers that are surrounded by cladding that has a refractive index (n_2) higher than that of the fiber itself (n_1) . This difference in refractive index causes total internal reflection and thus effectively delivers light from one end of the fiber to the other over long distances ranging from mm to even tens of km. 110 The flexibility of the fibers allows fluorescent sensors for corrosion to be placed in hard-to-reach areas to enable in situ observation. For example, Venancio et al. developed a novel corrosion fiber sensor based on 8-HQ that could be placed into the lap joints of an aluminum airframe and coupled the fiber to

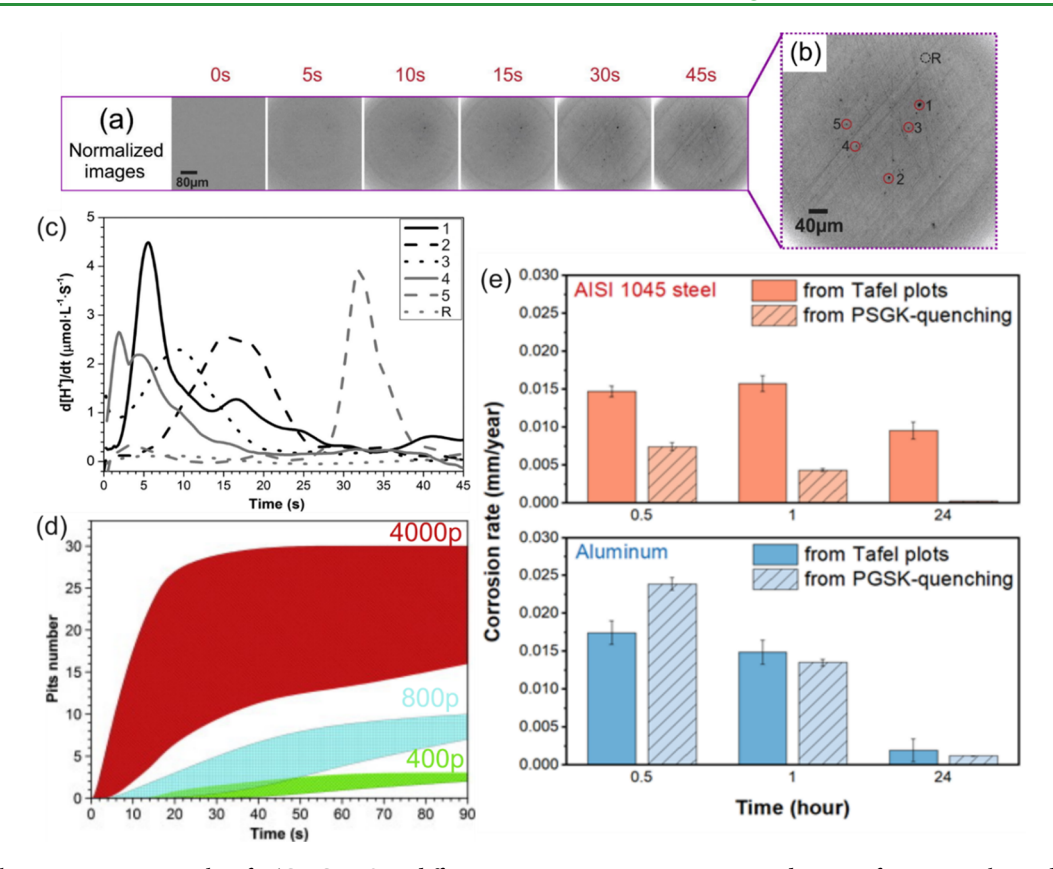


Figure 9. (a) Fluorescence micrographs of 56CF CHEQ at different time points on 4000-grit ground iron surfaces in an electrochemical cell. (b) Identified corrosion pits 1-5 circled in red along with a reference point (R). (c) Change in H⁺ concentration over time at the five spots found in (b) as quantified by correlating the fluorescent intensity to pH with a titration calibration. (d) Number of pits identified over time for three surface roughness obtained by 4000, 800, and 400 grit sandpaper. (a)–(d) adapted with permission from ref 55 Copyright 2014 Elsevier. (e) Comparison of corrosion rate (in mm/yr) found via PGSK fluorescence quenching and Tafel plot method for both AISI 1045 steel and aluminum. (e) reproduced from ref 67. Available under a CC-BY license. Copyright 2024 Liu, L.; Pfaffenberger, Z.; Siegel, M.; Saini, A.; Kisley, L.

an AvaSpec-2048 spectrometer. They correlated the fluorescent intensity to the concentration of Al $^{3+}$ and were able to detect concentrations down to 100 $\mu\rm M.^{111}$ The fiber tips in these studies are modified to introduce the fluorescent probe molecule to a local site. The fluorescent sensor may be covalently bound, embedded in, or imprinted onto a polymer that is coated on the distal fiber end, as seen in Figure 8. 56,109,111,112 Several other methods to affix the fluorescent sensor to the end of the fiber have been introduced such as covalently bonding or embedding in nylon membranes or hydrogels. 56,112

Several studies by David Walt's group have used a modified fiber to image local pH changes and metal ions quantitatively. 109,113 Using a fluorescein isothiocyanate (FITC) fluorescent sensor embedded in poly(acrylamide-co-N-acryloxysuccinimide) coated on a silanized fiber, the fluorescence intensity ratios at 490/440 nm excitation and 530 nm emission were correlated to the pH (Figure 8a). Higher ratios, or higher pH, are white, while the lower ratios, a lower pH, are black in the resulting image. The pH changes corresponded to visible corrosion areas found by bright field imaging (Figure 8b,c, red arrow). However, the fiber bundle consisted of 4 μ m diameter fibers, 113 resulting in the hexagonal pixelation observed in the fluorescence image (Figure 8b). In another study, the same group modified one fiber with SNAFL-SE (pH-sensitive) and another fiber with morin, an Al3+ chelator, to quantify the pH and ion concentration change with minute time resolution (Figure 8d,e). 109 This study was one of the few to

quantitatively assess how the change in fluorescence intensity correlated with the corrosion rates.

Optical fibers have the following advantages. (1) Attaching the fluorescent sensor to a fiber indirectly introduces the fluorescent molecule so the molecule itself is not perturbed by the environment or increases corrosion rates. (2) One can develop remote sensing with the distance enabled by the fiber which can access areas like airframes or steel bars in concrete. (3) The information is inherently localized when using fiber bundles and thus can report on localized corrosion such as pitting corrosion or crevice corrosion.

Optical fibers also have the following disadvantages for local corrosion detection. (1) Optical fiber bundles limit the lateral resolution of an image in the specimen plane to about twice the average core-to-core distance between fibers divided by the optical magnification of the imaging lenses (Figure 8b). 114 (2) Optical fiber bundles limit the field of view for imaging applications. Optical fibers can range from hundreds of micrometers to a few millimeters in diameter. 115 Optical fiber bundles are often employed with a scanning microscope to image larger areas or with single-mode fibers that essentially act as a confocal microscope enabling resolution at the diffraction limit. 115 In all the corrosion studies reviewed here and displayed in Figure 8, the fiber was not scanned to reconstruct a large image but instead simply placed at different locations at the sample/solution interface. (3) Optical fibers with corrosion sensors either have one-time use or must

undergo a cleaning procedure if the fluorescent sensor reaction is irreversible.

3.4. Current Methods Do Not Achieve the Spatiotemporal Resolution Needed to Study Early Pitting **Corrosion Stages.** In the majority of the work discussed thus far, the spatial and temporal scales measured by fluorescence analytical techniques have been only loosely quantified and are large, in comparison to the scales of localized corrosion. In the case of sensors in coatings, microscopic imaging has only been reported at length scales from 200 μ m to 2 mm with no specific, defined resolution. ^{98,100,105–107} In cases of optical fibers and solution-based detection, length scales reported have been from 10 to 40 μ m, again often without a specific resolution reported. The work of Walt et al. did report a 4 μ m resolution that was limited by the fiber bundle pixelation, as seen in Figure 8a. In all the different imaging modalities, the reported time scales for images have ranged from 2 min to weeks with minutes to hours between the reported imaging samples. Early corrosion stages like metastable pitting are submicrometer. 116 Maurice et al. found that metastable pits on nickel after 90 min of exposure to salt solution have a lateral size of 43 nm and a depth of 3 nm. 117 The depth of most corrosion pits are at the nanometer length scale. 70 Frankel observed the radius of a 2D aluminum pit to change by 125 μ m in 10 s at the pitting potential. Therefore, future studies of corrosion using fluorescence should work to obtain nanoscale spatial resolution with subsecond time resolution to resolve early-stage corrosion and pitting in real-time. Such information would help gain a mechanistic understanding of passive film breakdown and early corrosion pit nucleation and propagation.

For fluorescence sensing and imaging to gain acceptance by the corrosion community, it is important to contextualize the quantities measured by fluorescence within current research in the corrosion community. First, fluorescence techniques provide new data that would be inaccessible by traditional methods. Janet Wong's group has used the pH sensor 56CF delivered via solution in a quantitative microscopy study to assess the effects of surface roughness on corrosion rate with second-scale temporal resolution (Figure 9a). The 56CF decreases in fluorescence intensity at low pH (higher H⁺ concentration). This pH decrease is due to localized acidification at the anodic area within a pit (Figure 2ii). Therefore, black spots forming on the surface were attributed to corrosion pits observed in Figure 9a. The concentration of hydrogen ions in these individual corrosion pits was quantified, and local heterogeneity in concentration change rates was observed (Figure 9c). The authors were able to conclude that decreasing surface roughness led to faster pit formation at the early seconds-long time scale, as they saw a greater number of pits form in 90 s for a more polished surface, seen in Figure 9d. The Wong group's study highlights that fluorescence measurements can be performed in situ in a standard electrochemical cell to obtain information on localized corrosion that can be obtained at second and subsecond time scales to lead to new insights into known corrosion factors, such as surface roughness. Yet, their study was diffraction-limited as they used only a 20× objective with a low numerical aperture. The low spatial resolution prevented them from visualizing pit morphology and correlating that to the differences in hydrogen ion concentration observed to the nanoscale. Although they quantify the rate of hydrogen ion formation, they do not

compare their measurements to known information in the field on the pH expected in a corrosion pit.

Next, fluorescent sensors in corrosion can be contextualized by comparing rates measured by fluorescence to those measured by electrochemical techniques. We have recently addressed this gap by performing fluorometry of PGSK to develop a quantitative relationship between fluorescence intensity and the concentration of aluminum and iron ions produced by corrosion (Figure 5f).⁶⁷ By performing a titration experiment, the change in PGSK fluorescence intensity was converted to a concentration of Al3+ or Fe2+ ions. These concentrations could then be converted to a corrosion rate in mm/yr using known physical properties of the metal and solution. The fluorescence quenching observed rates were compared to rates measured under the same solution conditions using the established electrochemical method of Tafel plots in Figure 9e. A very strong agreement between methods were observed as the rates followed the same trends over time and had the same order of magnitude. This rate agreement is remarkable given the vastly different methods: PGSK senses the metal ions while the Tafel plot from electrochemical polarization test measures charge transfer. Additionally, the technique worked for both aluminum and iron, showing the high versatility of the method. The consistently lower rates observed in steel using the PGSK method can be attributed to different pathways in corrosion, such as Fe²⁺ being further reduced to Fe³⁺. This points to the limitation in bulk fluorometry techniques as it is difficult to distinguish different corrosion pathways from this kind of bulk measurement. Additionally, this study was done using bulk fluorimetry and thus lacked spatial information on the fluorescence turn-on. Other groups have recently applied microscale fluorescence microscopy of fluorescently labeled corrosion inhibitors with electrochemical polarization measurements to spatially resolve the preferential adsorption of sodium dodecyl sulfate to the α -Mg phase of LZ91 Mg-Li alloys. ¹¹⁹ Exploring and quantifying similar corrosion rates and inhibition mechanisms with nanoscale resolution are a topic of future work from our group.

4. QUANTITATIVE SPATIOTEMPORAL FLUORESCENCE MICROSCOPY AT THE SINGLE-MOLECULE SCALE

All corrosion detection microscopy discussed thus far is limited in resolution. The diffraction limit prevents achieving spatial resolutions smaller than approximately half the wavelength of light used to image a sample using conventional methods. 68 Light focuses into a point spread function (PSF) or Airy pattern, with a central peak surrounded by rings of a diffraction pattern. 120-122 The central peak width of such a pattern is typically 200-300 nm for visible microscopy, preventing resolutions below this scale and resolving individual molecules. However, interest in imaging beyond this size pushed for the development of new hardware and software methods to allow for workarounds to break the diffraction limit of light and image novel structures below 200 nm. 123-127 Features like proteins, nuclear pores, viruses, single fluorescent molecules (useful in detecting corrosion as discussed in sections 2 and 3), and various other structures found on the molecular scale have been analyzed with these super-resolution microscopy methods that overcome the diffraction limit of light. 128,129

SMLM can achieve imaging below the diffraction limit of light. ^{128–134} Individual signals from fluorophores will yield a

PSF spread on the camera detection surface. By fitting the data to an appropriate approximation of the PSF function, such as a 2D Gaussian, one can localize the peak of the signal generated. The localization allows for accurate reconstruction of where the fluorophore is on a scale smaller than that of the original diffraction-limited PSF resolution. Additionally, the possible overlap of different fluorophore molecules is circumvented through photoblinking, photoswitching, or adsorption, where fluorophores switch from "on" and "off" states where they intermittently fluoresce and go dark, or they move into and out of frame of the area of interest. 135 These stochastic processes allow for a smaller number of fluorophores to be on at any given time, making the total number of active fluorophores relatively low. This low density of active fluorophores makes it possible to spatially isolate individual fluorophore PSF signals and limits signal overlap between neighboring fluorophores that would complicate PSF fitting. After collecting the on/off events of an area over a long-time interval, typically on the scale of thousands of frames, these signals can then be combined to give a complete account of all single-molecule activity from a particular point, which can then be displayed in a new, higher resolution image on the typical order of 10s of nanometers.

4.1. SMLM Can Quantify Kinetic Information on Redox Reactions Absent in Ensemble Experiments. SMLM can access information about chemical kinetics at millisecond time scales. Particularly in the chemical catalysis community, SMLM has been effectively used to learn about the chemical kinetics of redox reactions. For example, Xu et al. determined that there are three distinct types of nanoparticles in the catalytic reduction of resazurin to resorufin. Specifically, they calculated differences in the on- (τ_{on}) and off- (τ_{off}) times of the fluorescent burst under a Langmuir–Hinshelwood framework for different single nanoparticles, yielding concentration and reaction rates of specific nanoparticles (Figure 10a-c). Through this method, they found a novel substrate-dependent desorption mechanism that could guide future catalyst design.

SMLM can also combine millisecond kinetic information with nanoscale position information to yield novel photocatalyst insights. ^{32,73,74} Shen et al. used the colocalization of a fluorescein probe—sensitive to OH radicals—and furyl alcohol—sensitive to Lewis acids—to show the tungsten nanowire catalysts could be treated with ascorbic acid to have more active sites (Figure 10d,e).

4.2. SMLM Can Image Fluorophores Activated by Corrosion, Displaying Properties Necessary for Analysis of Reaction Kinetics. Similar to the work in the catalysis community, SMLM analysis can be applied to corrosion redox reactions to provide temporal information. In our earlier report, Saini et al.²⁹ showed that the fluorophore resazurin reduction (Figure 3) can act as a corrosion detector at singlemolecule scales on a wide-field total internal reflection fluorescence (TIRF) microscope. Figure 11a depicts individual fluorophore turn-ons in the presence of the corrosion of Fe colloids over the course of a few hours, with the number of single-molecule events increasing linearly over time. The subsequent single-molecule photoblinking and/or reactions of resorufin at individually localized spatial sites have been observed on a millisecond time scale (Figure 11b). These observations show that single fluorophores activated by corrosion can be recorded in ideal SMLM conditions, allowing for localized corrosion sites to be analyzed on a single-

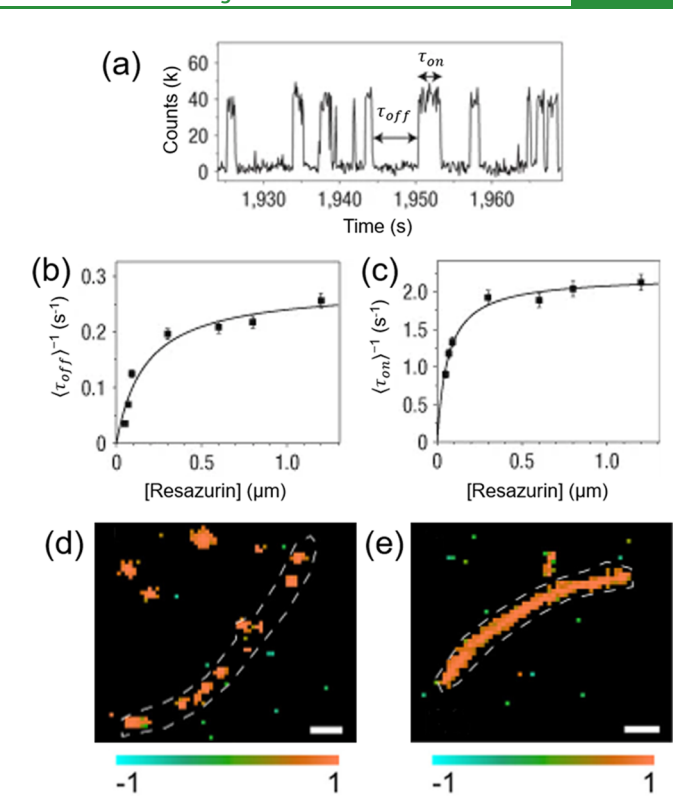


Figure 10. (a) Single-molecule photoblinking behaviors from a single resazurin molecule. (b) and (c) resazurin concentration dependence of fluorophore $\langle \tau_{off} \rangle^{-1}$ and $\langle \tau_{on} \rangle^{-1}$ respectively. (a)–(c) adapted with permission from ref 72. (a)–(c) Reproduced with permission from ref 72. Copyright 2008 Nature Publishing Group. Bottom images show furyl alcohol (FA) and 3'-(p-aminophenyl) fluorescein (APF) SMLM around tungsten wire before (d) and after (e) ascorbic acid treatment. Color scale reflects the colocalization score between the two probes. Scale bars are 1 μ m. (d) and (e) reproduced from ref 136. Copyright 2022 American Chemical Society.

molecule scale. Importantly, our single-molecule results show that the prior microscale fluorescence imaging of corrosion was only limited by the optical hardware capabilities. Using high-quality microscopy components such as laser excitation, a high numerical aperture objective, and a 95% quantum efficiency camera increases photon yield to allow us to detect corrosively turned-on resorufin at the single-molecule scale.

SMLM is uniquely suited to spatially resolve early pitting corrosion which occurs on the nanoscale.⁷⁰ Our group has demonstrated that resazurin can localize corrosion spatially on colloidal iron particles. Briefly, the same iron colloidal particles reported in Figure 11 were drop cast onto a coverslip and imaged on an Olympus IX83 microscope equipped with a 100×, NA 1.49 oil immersion objective under 561 nm excitation as detailed previously.²⁹ A solution of 300 mM NaCl and 20 nM resazurin was then pipetted on top of the colloid particles. A full description of the methods is provided in the Supporting Information. Bright fluorescent spots could be immediately observed on the perimeter of the iron particles (Figure 12a) and could be localized with a custom-written localization code. 137 These resulting images are displayed in Figure 12. Due to the geometry of the particle, sample substrate, and microscope, localizations were limited to the ring around the edge of the particle where dye solution could access and excitation light could reach within the ~100 nm axial distance of the total internal reflection geometry. Further

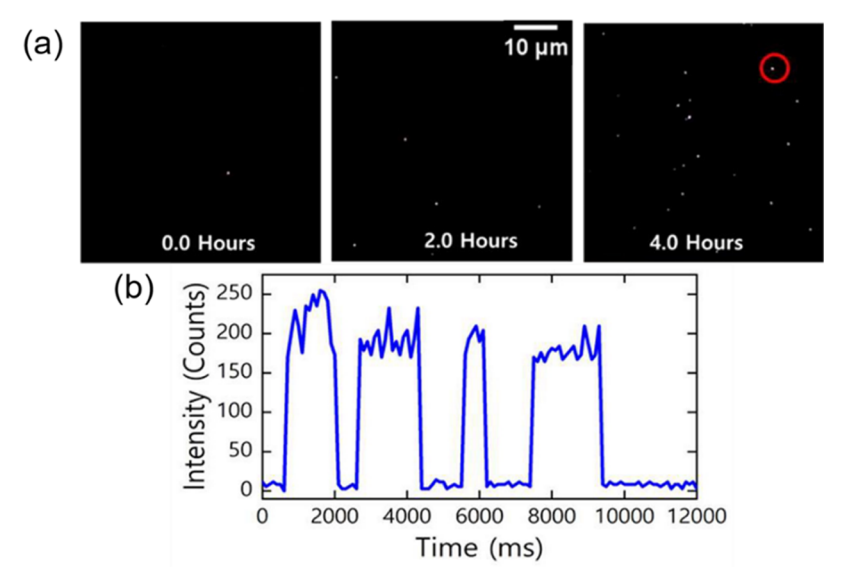


Figure 11. Single-molecule detection of resorufin in salt water over coverslips drop-casted with iron powder as viewed from a TIRF wide field microscope. (a) Snapshots of molecule "turn-on" over time at several time points over a 55 μ m² area. (b) Single-step photoblinking behavior over time of fluorophore circled in red in (a) provides evidence of single-molecule detection. Adapted from ref 29. Copyright 2020 American Chemical

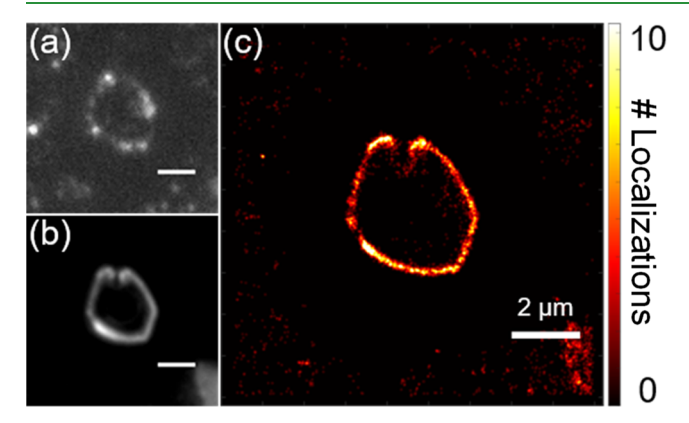


Figure 12. Localization data on single colloidal iron particle localization. (a) Single frame of unprocessed data taken of singular iron colloid. (b) Average diffraction limited intensity across full imaging time. (c) Super-resolution colloidal particle image after the single-molecule localization process, with color scheme displaying the number of localized molecules. Scale bars are 2 μ m.

work from our group is pursuing imaging of metal surfaces to provide more comprehensive spatial information, but Figure 12 is a preliminary demonstration of super-resolution fluorescence imaging of corrosion at a metal/solution interface.

Future SMLM analysis can be expanded upon by following inspiration from previously discussed catalysis research. The au_{on} and τ_{off} for resorufin can be measured to yield in situ average and local corrosion rates. The spatially localized rates can be correlated to bulk measurement from electrochemical techniques or weight loss methods to determine underlying heterogeneities within the averaged findings. Further studies can investigate the spatial distribution of anodic and cathodic corrosion reactions around corrosion pits under different conditions such as illumination, salt concentration, and passive film thickness using the range of fluorophores discussed in section 2 to help uncover how metal surfaces initiate pits and how they become vulnerable to corrosion in the long term.

5. CONCLUSION: OPPORTUNITIES TO SPATIOTEMPORALLY UNDERSTAND CORROSION USING FLUORESCENCE

This review has discussed different fluorescence-based corrosion detection methods and various ways that fluorescence techniques can be used to investigate the fundamentals of corrosion reactions. Bulk fluorescence tests are a fast way to get quantitative information about a corrosion system, and fluorescence microscopy can be used to analyze corrosion at a detailed spatial level. The application of singlemolecule microscopy provides an ideal platform for pushing fluorescence corrosion research further still, by combining nanometer scale spatial resolution with detailed quantitative information on corrosion dynamics on a subsecond time scale.

Corrosion research moving forward could focus on the quantitative SMLM approach to better understand the fundamentals of the corrosion mechanism such as the spatiotemporal correlation between anodic and cathodic sites locally at surfaces. Recent work using diffraction-limited reflectometry at aluminum surfaces, 138 and SMLM at catalytic nanoparticles, 89 have supported that "chemical communication"—where cooperative chemical reactions on one site can lead to reactions at a neighbor—can occur at metal/solution interfaces. SMLM offers the potential to pursue similar mechanistic insight at diverse metal-environmental interfaces relevant to corrosion. The combination of spatial and kinetic information could further help distinguish between proposed mechanisms of pitting corrosion initiation by passive film breakdown. 134 To achieve SMLM at a broad range of corrosion-relevant metal surfaces, challenges in sample and microscope geometry, dye diffusion, and the stochastic nature of pit formation must be overcome, but our group is actively developing methods to do so. Overall, instead of a macroscale approach of trial-and-error involving experiments that can take months at a time and yield little quantitative information, our molecular approach would allow researchers to build a more fundamental understanding of corrosion mechanisms in

relevant systems and use that understanding to design novel protection methods for corroding metals and alloys.

ASSOCIATED CONTENT

Supporting Information

The Supporting Information is available free of charge at https://pubs.acs.org/doi/10.1021/acsami.4c07800.

Additional experimental details, materials, and methods of single-molecule imaging of colloids in Figure 12 (PDF)

AUTHOR INFORMATION

Corresponding Author

Lydia Kisley — Department of Physics, Case Western Reserve University, Cleveland, Ohio 44106-7079, United States; Department of Chemistry, Case Western Reserve University, Cleveland, Ohio 44106-7079, United States; orcid.org/0000-0002-8286-5264; Email: lydia.kisley@case.edu

Authors

Mark Siegel — Department of Physics, Case Western Reserve University, Cleveland, Ohio 44106-7079, United States Lianlian Liu — Department of Physics, Case Western Reserve University, Cleveland, Ohio 44106-7079, United States; orcid.org/0000-0002-5182-6086

Zechariah Pfaffenberger – Department of Physics, Case Western Reserve University, Cleveland, Ohio 44106-7079, United States

Complete contact information is available at: https://pubs.acs.org/10.1021/acsami.4c07800

Notes

The authors declare no competing financial interest.

■ ACKNOWLEDGMENTS

Acknowledgment is made to the donors of the American Chemical Society Petroleum Research Fund for partial support of this research, along with the National Science Foundation Award #2142821 made through the CHE CSD program and the Lubrizol Innovation Prize Fund. The authors also thank Kisley Lab members for providing helpful discussion.

REFERENCES

- (1) El-Sherik, A. M. Trends in Oil and Gas Corrosion Research and Technologies: Production and Transmission; Woodhead Publishing, 2017.
- (2) McCafferty, E. Societal Aspects of Corrosion. In *Introduction to Corrosion Science*; McCafferty, E., Ed.; Springer: New York, 2010; pp 1–11. DOI: 10.1007/978-1-4419-0455-3 1.
- (3) Wasim, M.; Shoaib, S.; Mubarak, N. M.; Inamuddin; Asiri, A. M. Factors Influencing Corrosion of Metal Pipes in Soils. *Environ. Chem. Lett.* **2018**, *16* (3), 861–879.
- (4) Hou, Y.; Lei, D.; Li, S.; Yang, W.; Li, C.-Q. Experimental Investigation on Corrosion Effect on Mechanical Properties of Buried Metal Pipes. *Int. J. Corros.* **2016**, 2016, No. e5808372.
- (5) Mansfeld, F.; Tsai, S. Laboratory Studies of Atmospheric Corrosion—I. Weight Loss and Electrochemical Measurements. Corros. Sci. 1980, 20 (7), 853–872.
- (6) Du, G.; Li, J.; Wang, W. K.; Jiang, C.; Song, S. Z. Detection and Characterization of Stress-Corrosion Cracking on 304 Stainless Steel by Electrochemical Noise and Acoustic Emission Techniques. *Corros. Sci.* **2011**, 53 (9), 2918–2926.

- (7) Marinetti, S.; Vavilov, V. IR Thermographic Detection and Characterization of Hidden Corrosion in Metals: General Analysis. *Corros. Sci.* **2010**, 52 (3), 865–872.
- (8) Silva, M. Z.; Gouyon, R.; Lepoutre, F. Hidden Corrosion Detection in Aircraft Aluminum Structures Using Laser Ultrasonics and Wavelet Transform Signal Analysis. *Ultrasonics* **2003**, *41* (4), 301–305.
- (9) Khalili, P.; Cawley, P. The Choice of Ultrasonic Inspection Method for the Detection of Corrosion at Inaccessible Locations. *NDT E Int.* **2018**, *99*, 80–92.
- (10) Fanijo, E. O.; Thomas, J. G.; Zhu, Y.; Esquivel Guerrero, J.; Hosking, N. C.; Cai, W.; Michel, F. M.; Brand, A. S. Quantitative Measurement of Corrosion at the Nanoscale by in Situ Spectral Modulation Interferometry. *Mater. Charact.* **2022**, *189*, 111992.
- (11) Gharbi, O.; Ngo, K.; Turmine, M.; Vivier, V. Local Electrochemical Impedance Spectroscopy: A Window into Heterogeneous Interfaces. *Curr. Opin. Electrochem.* **2020**, 20, 1–7.
- (12) Mouanga, M.; Puiggali, M.; Tribollet, B.; Vivier, V.; Pébère, N.; Devos, O. Galvanic Corrosion between Zinc and Carbon Steel Investigated by Local Electrochemical Impedance Spectroscopy. *Electrochim. Acta* **2013**, *88*, 6–14.
- (13) Zhong, C.; Tang, X.; Cheng, Y. F. Corrosion of Steel under the Defected Coating Studied by Localized Electrochemical Impedance Spectroscopy. *Electrochim. Acta* **2008**, *53* (14), 4740–4747.
- (14) Yin, Y.; Niu, L.; Lu, M.; Guo, W.; Chen, S. In Situ Characterization of Localized Corrosion of Stainless Steel by Scanning Electrochemical Microscope. *Appl. Surf. Sci.* **2009**, 255 (22), 9193–9199.
- (15) Polcari, D.; Dauphin-Ducharme, P.; Mauzeroll, J. Scanning Electrochemical Microscopy: A Comprehensive Review of Experimental Parameters from 1989 to 2015. *Chem. Rev.* **2016**, *116* (22), 13234–13278.
- (16) Liu, S.; Wang, Y. Application of AFM in Microbiology: A Review. *Scanning* **2010**, 32 (2), 61–73.
- (17) Meisnar, M.; Lozano-Perez, S.; Moody, M.; Holland, J. Low-Energy EDX A Novel Approach to Study Stress Corrosion Cracking in SUS304 Stainless Steel via Scanning Electron Microscopy. *Micron* **2014**, *66*, 16–22.
- (18) Kang, K. W.; Pereda, M. D.; Canafoglia, M. E.; Bilmes, P.; Llorente, C.; Bonetto, R. Uncertainty Studies of Topographical Measurements on Steel Surface Corrosion by 3D Scanning Electron Microscopy. *Micron* 2012, 43 (2), 387–395.
- (19) Song, Z.; Xie, Z.-H. A Literature Review of in Situ Transmission Electron Microscopy Technique in Corrosion Studies. *Micron* **2018**, *112*, 69–83.
- (20) Dhole, G. S.; Gunasekaran, G.; Ghorpade, T.; Vinjamur, M. Smart Acrylic Coatings for Corrosion Detection. *Prog. Org. Coat.* **2017**, *110*, 140–149.
- (21) Lv, J.; Yue, Q.; Ding, R.; Li, W.; Wang, X.; Gui, T.; Zhao, X. Intelligent Anti-Corrosion and Corrosion Detection Coatings Based on Layered Supramolecules Intercalated by Fluorescent off-on Probes. *J. Taiwan Inst. Chem. Eng.* **2021**, *118*, 309–324.
- (22) Ayala, C. E.; Pérez, R. L.; Mathaga, J. K.; Watson, A.; Evans, T.; Warner, I. M. Fluorescent Ionic Probe for Determination of Mechanical Properties of Healed Poly(Ethylene-Co-Methacrylic Acid) Ionomer Films. ACS Appl. Polym. Mater. 2022, 4 (2), 832–841.
- (23) Que, E. L.; Domaille, D. W.; Chang, C. J. Metals in Neurobiology: Probing Their Chemistry and Biology with Molecular Imaging. *Chem. Rev.* **2008**, *108* (5), 1517–1549.
- (24) Carter, K. P.; Young, A. M.; Palmer, A. E. Fluorescent Sensors for Measuring Metal Ions in Living Systems. *Chem. Rev.* **2014**, *114* (8), 4564–4601.
- (25) Kumar, N. M.; Gruhs, P.; Casini, A.; Biedermann, F.; Moreno-Alcántar, G.; Picchetti, P. Electrochemical Detection of Drugs via a Supramolecular Cucurbit[7]Uril-Based Indicator Displacement Assay. *ACS Sens.* **2023**, *8* (7), 2525–2532.
- (26) Li, M.; Chen, T.; Gooding, J. J.; Liu, J. Review of Carbon and Graphene Quantum Dots for Sensing. ACS Sens. 2019, 4 (7), 1732–1748.

- (27) Lichtman, J. W.; Conchello, J.-A. Fluorescence Microscopy. Nat. Methods 2005, 2 (12), 910-919.
- (28) Gatland, Z.; Madrid, D.; Siegel, M.; Kisley, L. Reduction Reactions at Metal/Non-Aqueous Interfaces Can Be Sensed with the Turn-on Fluorophore Resazurin. Mater. Chem. Front. 2023, 7 (11), 2260-2265.
- (29) Saini, A.; Messenger, H.; Kisley, L. Fluorophores "Turned-On" by Corrosion Reactions Can Be Detected at the Single-Molecule Level. ACS Appl. Mater. Interfaces 2021, 13 (1), 2000-2006.
- (30) Saini, A.; Messenger, H.; Kisley, L. Single Molecule Detection of Fluorophores "Turned-on" by Corrosion Reactions. In 2021 Conference on Lasers and Electro-Optics (CLEO); 2021; pp 1-2.
- (31) Messenger, H.; Madrid, D.; Saini, A.; Kisley, L. Native Diffusion of Fluorogenic Turn-on Dyes Accurately Report Interfacial Chemical Reaction Locations. Anal. Bioanal. Chem. 2023, 415 (18), 4479-4486.
- (32) Shen, M.; Rackers, W. H.; Sadtler, B. Getting the Most out of Fluorogenic Probes: Challenges and Opportunities in Using Single-Molecule Fluorescence to Image Electro- and Photocatalysis. Chemical & Biomedical Imaging 2023, 1 (8), 692-715.
- (33) Hao, R.; Peng, Z.; Zhang, B. Single-Molecule Fluorescence Microscopy for Probing the Electrochemical Interface. ACS Omega **2020**, 5 (1), 89–97.
- (34) Kariyottu Kuniyil, M. J.; Padmanaban, R. Anti-Stokes Fluorescence and Nonlinear Optical Properties of the Functionalized Phenoxazine-Based Dye: A Computational Study. ChemistrySelect **2021**, 6 (42), 11706–11717.
- (35) Erlich, A. D.; Dogantzis, N. P.; Nubani, L. A.; Trifoi, L. A.; Hodgson, G. K.; Impellizzeri, S. Design and Engineering of a Dual-Mode Absorption/Emission Molecular Switch for All-Optical Encryption. Phys. Chem. Chem. Phys. 2021, 23 (44), 25152-25161.
- (36) Lee, H.; Kim, K.; Kang, C. M.; Choo, A.; Han, D.; Kim, J. In Situ Confocal Fluorescence Lifetime Imaging of Nanopore Electrode Arrays with Redox Active Fluorogenic Amplex Red. Anal. Chem. 2022, 95 (2), 1038-1046.
- (37) Liu, Y.; Zhang, K.; Tian, X.; Zhou, L.; Liu, J.; Liu, B. Quantitative Single-Particle Fluorescence Imaging Elucidates Semiconductor Shell Influence on Ag@TiO2 Photocatalysis. ACS Appl. Mater. Interfaces 2021, 13 (6), 7680-7687.
- (38) Chen, C.; Yu, M.; Tong, J.; Xiong, L.; Li, Y.; Kong, X.; Liu, J.; Li, S. A Review of Fluorescence Based Corrosion Detection of Metals. Corros. Commun. 2022, 6, 1-15.
- (39) Sundaresan, V.; Bohn, P. W. Acid-Base Chemistry at the Single Ion Limit. Chem. Sci. 2020, 11 (40), 10951-10958.
- (40) Wencel, D.; Abel, T.; McDonagh, C. Optical Chemical pH Sensors. Anal. Chem. 2014, 86 (1), 15-29.
- (41) Ma, L.; Ren, C.; Wang, J.; Liu, T.; Yang, H.; Wang, Y.; Huang, Y.; Zhang, D. Self-Reporting Coatings for Autonomous Detection of Coating Damage and Metal Corrosion: A Review. Chem. Eng. J. 2021, 421, 127854.
- (42) Calle, L. M.; Li, W. Microencapsulated Indicators and Inhibitors for Corrosion Detection and Control. Handbook of Smart Coatings for Materials Protection 2014, 370-422.
- (43) Sousa, I.; Quevedo, M. C.; Sushkova, A.; Ferreira, M. G.; Tedim, J. Chitosan Microspheres as Carriers for Ph-indicating Species in Corrosion Sensing. *Macromol. Mater. Eng.* **2020**, 305 (2), 1900662.
- (44) Lee, T. H.; Song, Y. K.; Park, S. H.; Park, Y. I.; Noh, S. M.; Kim, J. C. Dual Stimuli Responsive Self-Reporting Material for Chemical Reservoir Coating. Appl. Surf. Sci. 2018, 434, 1327-1335.
- (45) Galvão, T. L. P.; Sousa, I.; Wilhelm, M.; Carneiro, J.; Opršal, J.; Kukačková, H.; Špaček, V.; Maia, F.; Gomes, J. R. B.; Tedim, J.; Ferreira, M. G. S. Improving the Functionality and Performance of AA2024 Corrosion Sensing Coatings with Nanocontainers. Chem. Eng. J. 2018, 341, 526-538.
- (46) Han, J.; Burgess, K. Fluorescent Indicators for Intracellular Ph. Chem. Rev. 2010, 110 (5), 2709-2728.
- (47) Brasselet, S.; Moerner, W. e. Fluorescence Behavior of Single-Molecule pH-Sensors. Single Mol. 2000, 1 (1), 17–23.

- (48) Le Guern, F.; Mussard, V.; Gaucher, A.; Rottman, M.; Prim, D. Fluorescein Derivatives as Fluorescent Probes for pH Monitoring along Recent Biological Applications. Int. J. Mol. Sci. 2020, 21 (23), 9217.
- (49) Zhou, P.; Tang, Z.; Li, P.; Liu, J. Unraveling the Mechanism for Tuning the Fluorescence of Fluorescein Derivatives: The Role of the Conical Intersection and N π^* State. J. Phys. Chem. Lett. 2021, 12 (28), 6478-6485.
- (50) Theerasilp, M.; Crespy, D. Halochromic Polymer Nanosensors for Simple Visual Detection of Local Ph in Coatings. Nano Lett. 2021, 21 (8), 3604-3610.
- (51) Johnson, R. E.; Agarwala, V. S. Fluorescence Based Chemical Sensors For Corrosion Detection; OnePetro, 1997.
- (52) Alodan, M. A.; Smyrl, W. H. Detection of Localized Corrosion Using Fluorescence Microscopy. J. Electrochem. Soc. 1997, 144 (10), L282.
- (53) Johnson, R. E.; Durrett, M. G.; Agarwala, V. S. ICI, Intelligent Corrosion Indicator, and Its Use for the Early Detection of Corrosion on Aluminum Alloy Surfaces by Fluorescence; OnePetro, 2000.
- (54) Li, W.; Calle, L. M. Review Of pH and Electrochemical Responsive Materials For Corrosion Control Applications; OnePetro, 2008.
- (55) Liu, X.; Spikes, H.; Wong, J. S. S. In Situ pH Responsive Fluorescent Probing of Localized Iron Corrosion. Corros. Sci. 2014, 87, 118-126.
- (56) Nguyen, T. H.; Venugopala, T.; Chen, S.; Sun, T.; Grattan, K. T. V.; Taylor, S. E.; Basheer, P. A. M.; Long, A. E. Fluorescence Based Fibre Optic pH Sensor for the pH 10-13 Range Suitable for Corrosion Monitoring in Concrete Structures. Sens. Actuators B Chem. 2014, 191, 498-507.
- (57) Wang, J.; Wang, J.; Zhou, Q.; Li, Z.; Han, Y.; Song, Y.; Yang, S.; Song, X.; Qi, T.; Möhwald, H.; Shchukin, D.; Li, G. L. Adaptive Polymeric Coatings with Self-reporting and Self-healing Dual Functions from Porous Core-Shell Nanostructures. Macromol. Mater. Eng. 2018, 303 (4), 1700616.
- (58) Zhang, J.; Frankel, G. S. Corrosion-Sensing Behavior of an Acrylic-Based Coating System. Corrosion 1999, 55 (10), 957-967.
- (59) Bedair, M. A.; Elaryian, H. M.; Bedair, A. H.; Aboushahba, R. M.; El-Aziz S. Fouda, A. Novel Coumarin-Buta-1,3-Diene Conjugated Donor-Acceptor Systems as Corrosion Inhibitors for Mild Steel in 1.0 M HCl: Synthesis, Electrochemical, Computational and SRB Biological Resistivity. Inorg. Chem. Commun. 2023, 148, 110304.
- (60) Su, F.; Du, X.; Shen, T.; Qin, A.; Li, W. Aggregation-Induced Emission Luminogens Sensors: Sensitive Fluorescence 'Turn-On' Response for pH and Visually Chemosensoring on Early Detection of Metal Corrosion. Prog. Org. Coat. 2021, 153, 106122.
- (61) Formica, M.; Fusi, V.; Giorgi, L.; Micheloni, M. New Fluorescent Chemosensors for Metal Ions in Solution. Coord. Chem. Rev. 2012, 256 (1), 170-192.
- (62) Eivaz Mohammadloo, H.; Sarabi, A. A.; Roshan, Sh.; Eivaz Mohammadloo, A. 8-Hydroxyquinoline/Nanoclay Epoxy Nanocomposite as a Smart Coating for Early Corrosion Detection. Corros. Eng., Sci. Technol. 2021, 56 (8), 753-766.
- (63) Taheri, N.; Sarabi, A. A.; Roshan, S. Investigation of Intelligent Protection and Corrosion Detection of Epoxy-Coated St-12 by Redox-Responsive Microcapsules Containing Dual-Functional 8-Hydroxyquinoline. Prog. Org. Coat. 2022, 172, 107073.
- (64) Dhole, G. S.; Gunasekaran, G.; Naik, R.; Ghorpade, T.; Vinjamur, M. Fluorescence Based Corrosion Detecting Epoxy Coating. Prog. Org. Coat. 2020, 138, 105425.
- (65) Shekari, Z.; Younesi, H.; Heydari, A.; Tajbakhsh, M.; Chaichi, M. J.; Shahbazi, A.; Saberi, D. Fluorescence Chemosensory Determination of Cu2+ Using a New Rhodamine-Morpholine Conjugate. Chemosensors 2017, 5 (3), 26.
- (66) Li, S.; Zhang, H.; Liu, J. Preparation and Performance of Fluorescent Sensing Coating for Monitoring Corrosion of Al Alloy 2024. Trans. Nonferrous Met. Soc. China 2006, 16, s159-s164.
- (67) Liu, L.; Pfaffenberger, Z.; Siegel, M.; Saini, A.; Kisley, L. A Turn-Off Fluorescent Sensor for Metal Ions Quantifies Corrosion in an Organic Solvent. J. Electrochem. Soc. 2024, 171, 051502.

- (68) Abbe, E. Beiträge zur Theorie des Mikroskops und der mikroskopischen Wahrnehmung. Arch. Für Mikrosk. Anat. 1873, 9 (1), 413–468.
- (69) An, J.; Song, X.; Wan, W.; Chen, Y.; Si, H.; Duan, H.; Li, L.; Tang, B. Kinetics of the Photoelectron-Transfer Process Characterized by Real-Time Single-Molecule Fluorescence Imaging on Individual Photocatalyst Particles. ACS Catal. 2021, 11 (12), 6872–6882.
- (70) Guo, P.; La Plante, E. C.; Wang, B.; Chen, X.; Balonis, M.; Bauchy, M.; Sant, G. Direct Observation of Pitting Corrosion Evolutions on Carbon Steel Surfaces at the Nano-to-Micro- Scales. *Sci. Rep.* **2018**, *8* (1), 7990.
- (71) Cao, J.; Zhang, D.; Xu, W. Imaging the Electrochemical Reactions on Single-Particle by Single-Molecule Fluorescent Microscopy. *Curr. Opin. Electrochem.* **2023**, 41, 101360.
- (72) Xu, W.; Kong, J. S.; Yeh, Y.-T. E.; Chen, P. Single-Molecule Nanocatalysis Reveals Heterogeneous Reaction Pathways and Catalytic Dynamics. *Nat. Mater.* **2008**, *7* (12), 992–996.
- (73) Ristanović, Z.; Hofmann, J. P.; De Cremer, G.; Kubarev, A. V.; Rohnke, M.; Meirer, F.; Hofkens, J.; Roeffaers, M. B.; Weckhuysen, B. M. Quantitative 3D Fluorescence Imaging of Single Catalytic Turnovers Reveals Spatiotemporal Gradients in Reactivity of Zeolite H-ZSM-5 Crystals upon Steaming. *J. Am. Chem. Soc.* **2015**, *137* (20), 6559–6568.
- (74) Kubarev, A. V.; Janssen, K. P. F.; Roeffaers, M. B. J. Noninvasive Nanoscopy Uncovers the Impact of the Hierarchical Porous Structure on the Catalytic Activity of Single Dealuminated Mordenite Crystals. *ChemCatChem.* **2015**, 7 (22), 3646–3650.
- (75) Shreir, L. L. Corrosion: Metal/Environment Reactions; Newnes, 2013.
- (76) Augustyniak, A. In-Situ Early Detection of Metal Corrosion via "Turn-on" Fluorescence in "Smart" Epoxy Coatings. Ph.D. Dissertation, University of New Hampshire, Durham, NH, 2011.
- (77) Ohno, T.; Lichtin, N. N. Mechanistic Aspects of the Quenching of Triplet Methylene Blue by Organic Reductants. *J. Phys. Chem.* **1982**, *86* (3), 354–360.
- (78) Zhou, X.; Andoy, N. M.; Liu, G.; Choudhary, E.; Han, K.-S.; Shen, H.; Chen, P. Quantitative Super-Resolution Imaging Uncovers Reactivity Patterns on Single Nanocatalysts. *Nat. Nanotechnol.* **2012**, 7 (4), 237–241.
- (79) Han, K. S.; Liu, G.; Zhou, X.; Medina, R. E.; Chen, P. How Does a Single Pt Nanocatalyst Behave in Two Different Reactions? A Single-Molecule Study. *Nano Lett.* **2012**, *12* (3), 1253–1259.
- (80) Dong, B.; Pei, Y.; Zhao, F.; Goh, T. W.; Qi, Z.; Xiao, C.; Chen, K.; Huang, W.; Fang, N. In Situ Quantitative Single-Molecule Study of Dynamic Catalytic Processes in Nanoconfinement. *Nat. Catal.* **2018**, *1* (2), 135–140.
- (81) Dong, B.; Pei, Y.; Mansour, N.; Lu, X.; Yang, K.; Huang, W.; Fang, N. Deciphering Nanoconfinement Effects on Molecular Orientation and Reaction Intermediate by Single Molecule Imaging. *Nat. Commun.* **2019**, *10* (1), 4815.
- (82) Dong, B.; Mansour, N.; Pei, Y.; Wang, Z.; Huang, T.; Filbrun, S. L.; Chen, M.; Cheng, X.; Pruski, M.; Huang, W.; Fang, N. Single Molecule Investigation of Nanoconfinement Hydrophobicity in Heterogeneous Catalysis. *J. Am. Chem. Soc.* **2020**, *142* (31), 13305–13309.
- (83) Ha, J. W.; Ruberu, T. P. A.; Han, R.; Dong, B.; Vela, J.; Fang, N. Super-Resolution Mapping of Photogenerated Electron and Hole Separation in Single Metal-Semiconductor Nanocatalysts. *J. Am. Chem. Soc.* **2014**, *136* (4), 1398–1408.
- (84) Sambur, J. B.; Chen, T.-Y.; Choudhary, E.; Chen, G.; Nissen, E. J.; Thomas, E. M.; Zou, N.; Chen, P. Sub-Particle Reaction and Photocurrent Mapping to Optimize Catalyst-Modified Photoanodes. *Nature* **2016**, *530* (7588), 77–80.
- (85) Wu, S.; Lee, J.-K.; Lim, P. C.; Xu, R.; Zhang, Z. Super-Resolution Imaging of Photogenerated Charges on CdS/g-C 3 N 4 Heterojunctions and Its Correlation with Photoactivity. *Nanoscale* **2022**, *14* (14), 5612–5624.

- (86) Xu, W.; Jain, P. K.; Beberwyck, B. J.; Alivisatos, A. P. Probing Redox Photocatalysis of Trapped Electrons and Holes on Single Sb-Doped Titania Nanorod Surfaces. *J. Am. Chem. Soc.* **2012**, *134* (9), 3946–3949.
- (87) Zhou, X.; Choudhary, E.; Andoy, N. M.; Zou, N.; Chen, P. Scalable Parallel Screening of Catalyst Activity at the Single-Particle Level and Subdiffraction Resolution. *ACS Catal.* **2013**, 3 (7), 1448–1453.
- (88) Zhang, Y.; Lucas, J. M.; Song, P.; Beberwyck, B.; Fu, Q.; Xu, W.; Alivisatos, A. P. Superresolution Fluorescence Mapping of Single-Nanoparticle Catalysts Reveals Spatiotemporal Variations in Surface Reactivity. *Proc. Natl. Acad. Sci. U. S. A.* 2015, 112 (29), 8959–8964.
- (89) Zou, N.; Zhou, X.; Chen, G.; Andoy, N. M.; Jung, W.; Liu, G.; Chen, P. Cooperative Communication within and between Single Nanocatalysts. *Nat. Chem.* **2018**, *10* (6), 607–614.
- (90) Mao, X.; Liu, C.; Hesari, M.; Zou, N.; Chen, P. Super-Resolution Imaging of Non-Fluorescent Reactions via Competition. *Nat. Chem.* **2019**, *11* (8), 687–694.
- (91) Wang, W.-K.; Chen, J.-J.; Lou, Z.-Z.; Kim, S.; Fujitsuka, M.; Yu, H.-Q.; Majima, T. Single-Molecule and -Particle Probing Crystal Edge/Corner as Highly Efficient Photocatalytic Sites on a Single TiO2 Particle. *Proc. Natl. Acad. Sci. U. S. A.* **2019**, *116* (38), 18827—18833.
- (92) Mao, X.; Chen, P. Inter-Facet Junction Effects on Particulate Photoelectrodes. *Nat. Mater.* **2022**, *21* (3), 331–337.
- (93) Wang, N.; Tachikawa, T.; Majima, T. Single-Molecule, Single-Particle Observation of Size-Dependent Photocatalytic Activity in Au/TiO₂ Nanocomposites. *Chem. Sci.* **2011**, *2* (5), 891–900.
- (94) Tachikawa, T.; Yonezawa, T.; Majima, T. Super-Resolution Mapping of Reactive Sites on Titania-Based Nanoparticles with Water-Soluble Fluorogenic Probes. *ACS Nano* **2013**, *7* (1), 263–275.
- (95) Tachikawa, T.; Yamashita, S.; Majima, T. Evidence for Crystal-Face-Dependent Tio2 Photocatalysis from Single-Molecule Imaging and Kinetic Analysis. J. Am. Chem. Soc. 2011, 133 (18), 7197–7204.
- (96) Boldt, F.-M.; Heinze, J.; Diez, M.; Petersen, J.; Börsch, M. Real-Time pH Microscopy down to the Molecular Level by Combined Scanning Electrochemical Microscopy/Single-Molecule Fluorescence Spectroscopy. *Anal. Chem.* **2004**, *76* (13), 3473–3481.
- (97) Saini, A.; Gatland, Z.; Begley, J.; Kisley, L. Investigation of Fluorophores for Single-Molecule Detection of Anodic Corrosion Redox Reactions. MRS Commun. 2021, 11 (6), 804–810.
- (98) Augustyniak, A.; Tsavalas, J.; Ming, W. Early Detection of Steel Corrosion via "Turn-On" Fluorescence in Smart Epoxy Coatings. *ACS Appl. Mater. Interfaces* **2009**, *1* (11), 2618–2623.
- (99) Huo, K.; Zhang, J.; Lin, T.; Zhang, Y.; Liu, Y.; Liu, X. Colorimetric and Fluorescent Dual-Mode pH Sensor with PMIA as Substrate and CQDs as Probe for High Accuracy Detection of Full Range pH. *Dyes Pigments* **2023**, 219, 111574.
- (100) Fan, D.; Li, L.; Qi, K.; Chen, Z.; Qiu, Y.; Guo, X. pH-Responsive Fluorescent Metal-Organic Framework as a Functional Nanofiller for Smart Coatings. *Inorg. Chem.* **2023**, *62* (30), 11887–11896.
- (101) Zhao, X.; Yuan, Y.; Wei, Y.; Zhang, Z.; Zhang, Y. LDH-Based "Smart" Films for Corrosion Sensing and Protection. *Materials* **2023**, *16* (9), 3483.
- (102) Henriques, R. R.; Carelo, J. C.; Soares, B. G. Anti-Corrosive and Self-Healing Properties of Epoxy Coatings Loaded with Montmorillonite Modified with Zinc-Based Ionic Liquid. *Prog. Org. Coat.* **2024**, *187*, 108185.
- (103) Feng, H.; Wang, T.; Wang, W.; Ma, C.; Pu, Y.; Chen, S. High Efficiency Photothermal Cyclic Self-Healing Antibacterial Coating Based on in-Situ Dual-Functional BiOI@Bi2S3. *J. Mater. Sci. Technol.* **2024**, *173*, 121–136.
- (104) Feng, H.; Wang, T.; Cao, L.; Pu, Y.; Zhao, Z.; Chen, S. Recent Achievements and Applications of Photothermal Self-Healing Coatings: A Review. *Prog. Org. Coat.* **2024**, *187*, 108153.
- (105) Exbrayat, L.; Salaluk, S.; Uebel, M.; Jenjob, R.; Rameau, B.; Koynov, K.; Landfester, K.; Rohwerder, M.; Crespy, D. Nanosensors

- for Monitoring Early Stages of Metallic Corrosion. ACS Applied Nano Materials 2019, 2 (2), 812-818.
- (106) Roshan, S.; Sarabi Dariani, A. A.; Mokhtari, J. Monitoring Underlying Epoxy-Coated St-37 Corrosion via 8-Hydroxyquinoline as a Fluorescent Indicator. Appl. Surf. Sci. 2018, 440, 880-888.
- (107) Eivaz Mohammadloo, H.; Mirabedini, S. M.; Pezeshk-Fallah, H. Microencapsulation of Quinoline and Cerium Based Inhibitors for Smart Coating Application: Anti-Corrosion, Morphology and Adhesion Study. Prog. Org. Coat. 2019, 137, 105339.
- (108) Panova, A. A.; Pantano, P.; Walt, D. R. In Situ Fluorescence Imaging of Localized Corrosion with a pH-Sensitive Imaging Fiber. Anal. Chem. 1997, 69 (8), 1635-1641.
- (109) Szunerits, S.; Walt, D. R. Aluminum Surface Corrosion and the Mechanism of Inhibitors Using pH and Metal Ion Selective Imaging Fiber Bundles. Anal. Chem. 2002, 74 (4), 886-894.
- (110) Addanki, S.; Amiri, I. S.; Yupapin, P. Review of Optical Fibers-Introduction and Applications in Fiber Lasers. Results Phys. 2018, 10, 743 - 750.
- (111) Venancio, P. G.; Cottis, R. A.; Narayanaswamy, R.; Fernandes, J. C. S. Optical Sensors for Corrosion Detection in Airframes. Sens. Actuators B Chem. 2013, 182, 774-781.
- (112) Bartelmess, J.; Zimmek, D.; Bartholmai, M.; Strangfeld, C.; Schäferling, M. Fibre Optic Ratiometric Fluorescence pH Sensor for Monitoring Corrosion in Concrete. Analyst 2020, 145 (6), 2111-
- (113) Bronk, K. S.; Michael, K. L.; Pantano, P.; Walt, D. R. Combined Imaging and Chemical Sensing Using a Single Optical Imaging Fiber. Anal. Chem. 1995, 67 (17), 2750-2757.
- (114) Chang, Y.; Lin, W.; Cheng, J.; Chen, S. C. Compact High-Resolution Endomicroscopy Based on Fiber Bundles and Image Stitching. Opt. Lett. 2018, 43 (17), 4168-4171.
- (115) Flusberg, B. A.; Cocker, E. D.; Piyawattanametha, W.; Jung, J. C.; Cheung, E. L. M.; Schnitzer, M. J. Fiber-Optic Fluorescence Imaging. Nat. Methods 2005, 2 (12), 941-950.
- (116) Frankel, G. S. Pitting Corrosion of Metals: A Review of the Critical Factors. J. Electrochem. Soc. 1998, 145 (6), 2186.
- (117) Maurice, V.; Klein, L. H.; Marcus, P. Atomic Structure of Metastable Pits Formed on Nickel. Electrochem. Solid-State Lett. 2001, 4 (1), B1.
- (118) Frankel, G. S. The Growth of 2-D Pits in Thin Film Aluminum. Corros. Sci. 1990, 30 (12), 1203-1218.
- (119) Chen, Y.; Xia, G.; Yan, H.; Xin, Y.; Song, H.; Luo, C.; Guan, H.; Luc, C.; Hu, Z. Visualising the Adsorption Behaviour of Sodium Dodecyl Sulfate Corrosion Inhibitor on the Mg Alloy Surface by a Novel Fluorescence Labeling Strategy. Appl. Surf. Sci. 2024, 642,
- (120) Rossmann, K. Point Spread-Function, Line Spread-Function, and Modulation Transfer Function. Radiology 1969, 93 (2), 257-272. (121) Nasse, M. J.; Woehl, J. C. Realistic Modeling of the Illumination Point Spread Function in Confocal Scanning Optical Microscopy. JOSA A 2010, 27 (2), 295-302.
- (122) Zhang, B.; Zerubia, J.; Olivo-Marin, J.-C. Gaussian Approximations of Fluorescence Microscope Point-Spread Function Models. Appl. Opt. 2007, 46 (10), 1819-1829.
- (123) Moerner, W. E.; Kador, L. Optical Detection and Spectroscopy of Single Molecules in a Solid. Phys. Rev. Lett. 1989, 62 (21), 2535-2538.
- (124) Egner, A.; Hell, S. W. Fluorescence Microscopy with Super-Resolved Optical Sections. Trends Cell Biol. 2005, 15 (4), 207-215.
- (125) Betzig, E.; Trautman, J. K. Near-Field Optics: Microscopy, Spectroscopy, and Surface Modification beyond the Diffraction Limit. Science 1992, 257 (5067), 189-195.
- (126) Ji, N.; Shroff, H.; Zhong, H.; Betzig, E. Advances in the Speed and Resolution of Light Microscopy. Curr. Opin. Neurobiol. 2008, 18 (6), 605-616.
- (127) Huang, B.; Bates, M.; Zhuang, X. Super-Resolution Fluorescence Microscopy. Annu. Rev. Biochem. 2009, 78 (1), 993-1016.

- (128) Donnert, G.; Keller, J.; Medda, R.; Andrei, M. A.; Rizzoli, S. O.; Lührmann, R.; Jahn, R.; Eggeling, C.; Hell, S. W. Macromolecular-Scale Resolution in Biological Fluorescence Microscopy. Proc. Natl. Acad. Sci. U. S. A. 2006, 103 (31), 11440-11445.
- (129) Schermelleh, L.; Ferrand, A.; Huser, T.; Eggeling, C.; Sauer, M.; Biehlmaier, O.; Drummen, G. P. C. Super-Resolution Microscopy Demystified. Nat. Cell Biol. 2019, 21 (1), 72-84.
- (130) Lelek, M.; Gyparaki, M. T.; Beliu, G.; Schueder, F.; Griffié, J.; Manley, S.; Jungmann, R.; Sauer, M.; Lakadamyali, M.; Zimmer, C. Single-Molecule Localization Microscopy. Nat. Rev. Methods Primer 2021. 1 (1). 1-27.
- (131) Heilemann, M.; van de Linde, S.; Schüttpelz, M.; Kasper, R.; Seefeldt, B.; Mukherjee, A.; Tinnefeld, P.; Sauer, M. Subdiffraction-Resolution Fluorescence Imaging with Conventional Fluorescent Probes. Angew. Chem., Int. Ed. 2008, 47 (33), 6172-6176.
- (132) Rust, M. J.; Bates, M.; Zhuang, X. Sub-Diffraction-Limit Imaging by Stochastic Optical Reconstruction Microscopy (STORM). Nat. Methods 2006, 3 (10), 793-796.
- (133) Hess, S. T.; Girirajan, T. P. K.; Mason, M. D. Ultra-High Resolution Imaging by Fluorescence Photoactivation Localization Microscopy. Biophys. J. 2006, 91 (11), 4258-4272.
- (134) Betzig, E.; Patterson, G. H.; Sougrat, R.; Lindwasser, O. W.; Olenych, S.; Bonifacino, J. S.; Davidson, M. W.; Lippincott-Schwartz, J.; Hess, H. F. Imaging Intracellular Fluorescent Proteins at Nanometer Resolution. Science 2006, 313 (5793), 1642-1645.
- (135) Sharonov, A.; Hochstrasser, R. M. Wide-Field Subdiffraction Imaging by Accumulated Binding of Diffusing Probes. Proc. Natl. Acad. Sci. U. S. A. 2006, 103 (50), 18911-18916.
- (136) Shen, M.; Ding, T.; Tan, C.; Rackers, W. H.; Zhang, D.; Lew, M. D.; Sadtler, B. In Situ Imaging of Catalytic Reactions on Tungsten Oxide Nanowires Connects Surface-Ligand Redox Chemistry with Photocatalytic Activity. Nano Lett. 2022, 22 (12), 4694-4701.
- (137) Kisley Research Group @ CWRU. GitHub DOI: 10.5281/ zenodo.10048387. https://github.com/KisleyLabAtCWRU (accessed Spring 2024).
- (138) Godeffroy, L.; Makogon, A.; Gam Derouich, S.; Kanoufi, F.; Shkirskiy, V. Imaging and Quantifying the Chemical Communication between Single Particles in Metal Alloys. Anal. Chem. 2023, 95 (26), 9999-10007.